

Cell & Bioscience

Epigenetic alterations in TRAMP mice: epigenome DNA methylation profiling using MeDIP-seq --Manuscript Draft--

Manuscript Number:	CBIO-D-17-00137R1	
Full Title:	Epigenetic alterations in TRAMP mice: epigenome DNA methylation profiling using MeDIP-seq	
Article Type:	Research	
Section/Category:	Genetics, Epigenetics and Genomics	
Funding Information:	National Center for Complementary and Integrative Health (R01-AT009152)	Prof. Ah-Ng Tony Kong
Abstract:	<p>Abstract Purpose: We investigated the genomic DNA methylation profile of prostate cancer in transgenic adenocarcinoma of the mouse prostate (TRAMP) cancer model and to analyze the crosstalk among targeted genes and the related functional pathways.</p> <p>Methods: Prostate DNA samples from 24-week-old TRAMP and C57BL/6 male mice were isolated. The DNA methylation profiles were analyzed by methylated DNA immunoprecipitation (MeDIP) followed by next-generation sequencing (MeDIP-seq). Canonical pathways, diseases & function and network analyses of the different samples were then performed using the Ingenuity® Pathway Analysis (IPA) software. Some target genes with significant difference in methylation were selected for validation using Methylation Specific Primers (MSP) and qPCR.</p> <p>Results: TRAMP mice undergo extensive aberrant CpG hyper- and hypo-methylation. There were 2,147 genes with a significant ($\log_2\text{-change} \geq 2$) change in CpG methylation between the two groups, as mapped by the IPA software. Among these genes, the methylation of 1,105 and 1,042 genes was significantly decreased and increased, respectively, in TRAMP prostate tumors. The top associated disease identified by IPA was adenocarcinoma; however, the cAMP response element-binding protein (CREB)-, Histone Deacetylase 2 (HDAC2)-, glutathione S-transferase pi (GSTP1)- and Polyubiquitin-C (UBC)-related pathways showed significantly altered methylation profiles based on the canonical pathway and network analyses. MSP and qPCR results of genes of interests corroborated with MeDIP-seq findings.</p> <p>Conclusions: This is the first MeDIP-seq with IPA analysis of the TRAMP model to provide novel insight into the genome-wide methylation profile of prostate cancer. Studies on epigenetics, such as DNA methylation, will potentially provide novel avenues and strategies for further development of biomarkers targeted for treatment and prevention approaches for prostate cancer.</p> <p>Keywords: MeDIP-seq, Epigenetics, DNA methylation, TRAMP, Prostate Cancer</p>	
Corresponding Author:	Ah-Ng Tony Kong Rutgers The State University of New Jersey Piscataway, NJ UNITED STATES	
Corresponding Author Secondary Information:		
Corresponding Author's Institution:	Rutgers The State University of New Jersey	
Corresponding Author's Secondary Institution:		
First Author:	Wenji Li	
First Author Secondary Information:		
Order of Authors:	Wenji Li	

	Ying Huang Davit Sargsyan Tin Oo Khor Yue Guo Limin Shu Anne Yuqing Yang Chengyue Zhang Ximena Paredes-Gonzalez Michael Verzi Ronald P Hart Ah-Ng Tony Kong
Order of Authors Secondary Information:	
Response to Reviewers:	<p>Response to Reviewer's Comment:</p> <p>Reviewer #1: The authors in this manuscript analyzed DNA methylation profiles in prostate tissues from 24-weeks old of TRAMP mice and age-matched C57BL/6 control mice by methylated DNA immunoprecipitation followed by next-generation sequencing and bioinformatics analyses. The study identified a significant alteration of methylation profiles in CREB-, HDAC2-, GSTP1- and UBC-related pathways in mouse prostate tumor tissues vs. normal tissues. The study is new and experimental methods were well described. There are some minor concerns which may help improve the overall quality of the study.</p> <p>1) Full names of genes should be given at the first appearance of their abbreviation. Response: Thank you for your suggestion. All the full gene names have been listed where they first appear.</p> <p>2) The authors need to clarify which part (s) of the mouse prostate were used for the methylation study. Response: We homogenized the whole prostate tissue and extracted and purified DNA. We did not separate different lobes. The modification has been made in page 5 Ln 111.</p> <p>3) The authors may discuss what percentages of high-grade prostatic hyperplasia and adenocarcinomas in each sample from the TRAMMP mice. Also, how stroma components affect the results? Response: This is a good question. According to reference Animal Models of Human Disease - Page 11, the autochthonous TRAMP model, The TRAMP mice develop early prostatic intraepithelial neoplasia (PIN) by 6 weeks, and mild- to high-grade PIN by 12 weeks. At 24 weeks, approximately 100% of male mice have poorly differentiated and invasive adenocarcinomas. Hence we selected 24 weeks as an end point to compare to see the maximum difference. The TRAMP mice used for our MeDIP-Seq analysis were randomly selected from a group of 14 mice. The group was fully characterized considering incidence of palpable tumor and metastases (Paredes-Gonzalez X et al, submitted). At 24 weeks of age, nearly 60% of the mice developed palpable prostate tumors, and one mice developed lymph node metastases (evaluated at necropsy). The dorsolateral prostates of seven TRAMP animals of the group were subjected to H&E staining to observe the neoplastic changes. They were evaluated by an independent pathologist in a blinded manner to classify the prostatic PIN (I to IV). Histological analyses revealed PIN was observed in all TRAMP models, among them more than 50% of the animals exhibited LG-PIN and more than 30% HG-PIN (Paredes-Gonzalez X et al, submitted). The three TRAMP mice randomly selected from the characterized group were matched by age with three wild type C57BL/6 mice (maintained under similar conditions during the study). It is well known that reactive stroma or carcinoma-associated fibroblasts can influence epithelial tumor progression. In prostate cancer (PCa), the amount of reactive stroma is variable and has predictive value for tumor recurrence. TRAMP mice have a very distinct stroma composition comparing with the WT. In our method, we homogenized</p>

the whole prostate tissue hence it is not possible to compare influence of stroma difference in gene methylation. It is meaningful to compare the methylation/RNA expression difference in stromas in the animal model. We would propose future study considering your valuable suggestions.

Reviewer #2: In this study, Kong and colleagues have investigated the genomic DNA methylation profile of prostate cancer in TRAMP cancer model and analyzed the crosstalk among targeted genes and the related functional pathways. Employing state-of-the-art techniques and cutting-edge analyses tools, the authors found that TRAMP mice undergo extensive aberrant CpG hyper- and hypo-methylation, providing novel insight into the genome-wide methylation profile of prostate cancer. These finding of the authors will potentially provide novel avenues and strategies for further development of biomarkers targeted for treatment and prevention approaches for prostate cancer. Overall, this is an elegant piece of work where the studies are logically designed and performed, and the results shown are very clear and convincing to support the conclusions drawn. It should be published in its present form.

Response: Thank you for your comments.

Reviewer #3: Wenji Li et al report on the DNA methylation profile changes of prostate cancer cells in a murine transgenic prostate adenocarcinoma compared to C57 black male background. They did pathway analysis on the results to identify canonical pathways that might be affected. The analysis revealed about 2K changes at the four fold level, with about half down and half up. Certain prime candidate emerged. Amongst them analysis of the HDAC2 and GSTP1 pathways revealed an intersection at TP53. This showed consistency of the TRAMP model and clinical studies, which is important to establishing the fidelity of the SV40 T driven TRAMP tumor to naturally occurring disease. These studies are logically conceived and well executed. The data analysis is thorough and logically done. The conclusions are fully justified. The introduction and discussion are nicely written synopsis, motivating and summarizing the study. The schematic is a nice aid, too. This is a valuable contribution to the literature and acceptance is recommended.

There are some minor things that the authors may wish to give consideration to - none of which affect suitability for publication.

Ln. 72, CpG is probably meant instead of CGI

Response: Thanks for your remind. It has been changed to CpG island in new Ln 73.

Ln 93, were is probably not meant to be in that sentence.

Response: "were" has been changed to "was" in new Ln96.

Ln 102 weighed is probably meant instead of weighted

Response: "Weighted" has been changed to "weighed" in new Ln 105.

Ln 230 interesting is probably meant instead of interested

Response: "Interested" has been changed to "Interesting" in new LN 227.

Response to Editor's comments:

We have polished the English grammar and structure and reduced the potential similarity with published papers using Turnitin.

[Click here to view linked References](#)

1

Epigenetic alterations in TRAMP mice: epigenome DNA methylation profiling using MeDIP-seq

Wenji Li ^{a,b,1}, Ying Huang ^{a,b,c,1}, Davit Sargsyan^{a,b,c}, Tin Oo Khor ^{a,b}, Yue Guo ^{a,b,c}, Limin Shu ^{a,b}, Anne Yuqing Yang^{a,b,c}, Chengyue Zhang^{a,b,c}, Ximena Paredes-Gonzalez ^{a,b,c}, Michael Verzi ^d, Ronald P Hart ^e, and Ah-Ng Kong ^{a,b,*}

^aCenter for Phytochemical Epigenome Studies, Ernest Mario School of Pharmacy, The State University of New Jersey, Piscataway, NJ 08854, USA.

^bDepartment of Pharmaceutics, Ernest Mario School of Pharmacy, The State University of New Jersey, Piscataway, NJ 08854, USA.

^cGraduate Program in Pharmaceutical Sciences, Ernest Mario School of Pharmacy, The State University of New Jersey, Piscataway, NJ 08854, USA.

^dDepartment of Genetics, The State University of New Jersey, Piscataway, NJ 08854, USA.

^aDepartment of Cell Biology and Neuroscience, Rutgers, The State University of New Jersey, Piscataway, NJ 08854, USA.

¹Equal contribution

*Correspondence should be addressed to:
Professor Ah-Ng Tony Kong
Rutgers, The State University of New Jersey
Ernest Mario School of Pharmacy, Room 228
160 Frelinghuysen Road,
Piscataway, NJ 08854, USA
Email: kongt@pharmacy.rutgers.edu
Phone: 848-445-6369/8
Fax: 732-445-3134

Abstract

Purpose: We investigated the genomic DNA methylation profile of prostate cancer in transgenic adenocarcinoma of the mouse prostate (TRAMP) cancer model and to analyze the crosstalk among targeted genes and the related functional pathways.

Methods: Prostate DNA samples from 24-week-old TRAMP and C57BL/6 male mice were isolated. The DNA methylation profiles were analyzed by methylated DNA immunoprecipitation (MeDIP) followed by next-generation sequencing (MeDIP-seq). Canonical pathways, diseases & function and network analyses of the different samples were then performed using the Ingenuity® Pathway Analysis (IPA) software. Some target genes with significant difference in methylation were selected for validation using Methylation Specific Primers (MSP) and qPCR.

Results: TRAMP mice undergo extensive aberrant CpG hyper- and hypo-methylation. There were 2,147 genes with a significant ($\log_2\text{-change} \geq 2$) change in CpG methylation between the two groups, as mapped by the IPA software. Among these genes, the methylation of 1,105 and 1,042 genes was significantly decreased and increased, respectively, in TRAMP prostate tumors. The top associated disease identified by IPA was adenocarcinoma; however, the **cAMP response element-binding protein (CREB)-, Histone Deacetylase 2 (HDAC2)-, glutathione S-transferase pi (GSTP1)- and Polyubiquitin-C (UBC)-**related pathways showed significantly altered methylation profiles based on the canonical pathway and network analyses. MSP and qPCR results of **genes of interests** corroborated with MeDIP-seq findings.

Conclusions: This is the first MeDIP-seq with IPA analysis of the TRAMP model to provide novel insight into the genome-wide methylation profile of prostate cancer. Studies on epigenetics, such as DNA methylation, will potentially provide novel avenues and strategies for further development of biomarkers targeted for treatment and prevention approaches for prostate cancer.

Keywords: MeDIP-seq, Epigenetics, DNA methylation, TRAMP, Prostate Cancer

Introduction

Prostate cancer is the **second leading male cancer** (accounts for 13.8% of all male cancers) and its prevalence ranking number five among all cancers [1]. In the United States, prostate cancer is the most common male cancer subtype, apart from non-melanoma skin cancer [2]. Prostate cancer is a clinically heterogeneous disease with marked variability in patient outcomes [3]. Early detection, accurate prediction and successful management of prostate cancer represent some of the most challenging and controversial issues [4]. Interestingly, epigenetic changes are hallmarks of prostate cancer, among which DNA methylation is the most frequently studied [5].

Epigenetic changes include DNA methylation, histone modification, and posttranslational gene regulation by micro-RNAs (miRNAs) [6]. Among these, DNA methylation has been well studied, and aberrant DNA methylation patterns are a characteristic feature of cancer [7-9]. The first reported epigenetic changes in human cancer were DNA methylation losses. Since then, genomic hypomethylation has been found to be associated with multiple cancer types [10, 11]. In addition, hypermethylation of CpG islands (CGIs) at promoters of tumor suppressor genes, homeobox genes and other sequences are other consistent epigenetic features of cancer [12, 13]. **CpG island methylator-phenotype (CIMP)** tumors have been identified in many cancers, including oral cancer, colorectal cancer [14] and colon cancer [15]. Therefore, it is worthwhile to profile the global DNA methylation changes between cancer models and controls to elucidate the mechanisms of carcinogenesis.

The transgenic adenocarcinoma of the mouse prostate (TRAMP) model closely represents the pathogenesis of human prostate cancer because male TRAMP mice spontaneously develop autochthonous prostate tumors following the onset of puberty [16] and it specifically induces transgene expression in the prostate, displays distant organ metastases and it has castration-resistant properties [17]. DNA methylation in the TRAMP model has been widely studied *in vitro* and *in vivo*, resulting in the discovery of the methylated markers **Nuclear factor (erythroid-derived 2)-like 2(NRF2)** [18], **O6-alkylguanine DNA alkyltransferase (MGMT)** [19], **glutathione S-transferase pi (GSTP1)** [20], **14-3-3σ** [21], and **Krueppel-like factor 6 (KLF6)** [22].

1
2
3
4 85 However, only Shannon et al have compared global methylation alteration among TRAMP and
5
6 86 wild type (WT) mice [23]. Systemic comparisons and analyses of the genomic methylation status of
7
8 87 prostate cancer models and normal controls are needed to determine the underlying interactions between
9
10 88 these target genes and to discover new biomarkers. We are the first to perform methylated DNA
11
12 89 immunoprecipitation (MeDIP) coupled with next-generation sequencing (MeDIP-seq) followed by
13
14 90 Ingenuity® Pathway Analysis (IPA) studies to investigate the crosstalk among important genes and to
15
16 91 analyze overlapping functional pathways by comparing the whole genomic DNA methylation patterns
17
18 92 between the TRAMP model and controls.
19
20
21
22 93
23
24 94
25
26 95 **Materials and methods**
27
28 96 **Genomic DNA extraction from TRAMP and C57BL/6 male mice**
29
30 96 The breeding of TRAMP mice was followed our previous publication [24, 25]. Briefly, female
31
32 97 hemizygous C57BL/TGN TRAMP mice, line PB Tag 8247NG (Jackson Laboratory, Bar Harbor, ME),
33
34 98 were bred with the same genetic background male C57BL/6 mice (Jackson Laboratory, Bar Harbor, ME).
35
36 99 Identity of transgenic mice was established by PCR-based DNA genotyping using the primers suggested
37
38 100 by The Jackson Laboratory as we previously described [24, 25]. F1 (first generation from cross breeding)
39
40 101 or F2 (second generation from cross breeding) male TRAMP mice were used for the studies. Mice were
41
42 102 housed in cages containing wood-chip bedding in a temperature-controlled room (20–22°C) with a 12-h-
43
44 103 light/dark cycle and a relative humidity of 45–55% at Rutgers Animal Care Facility. All animals received
45
46 104 water and food *ad libitum* until sacrifice (24 weeks of age) by carbon dioxide euthanasia. The study was
47
48 105 performed using an IACUC-approved protocol (01-016) at Rutgers University. Mice were weighed and
49
50 106 evaluated in the overall health twice weekly during all the study. Presences of palpable tumor, metastases,
51
52 107 genitourinary (GU) apparatus weight were evaluated upon necropsy and prostate intraepithelial neoplasia
53
54 108 lesions (evaluated by H&E staining) were monitored in the TRAMP group (data not shown). Prostate
55
56 109 samples from three 24-week-old TRAMP and three 24 weeks old C57BL/6 mice (maintained under
57
58 110 similar conditions) were randomly selected out. A DNeasy Kit (Qiagen, Valencia, CA, USA) was used to
59
60
61
62
63
64
65

1
2
3
4 111 extract the genomic DNA (gDNA) from **whole** prostate samples of three 24-week-old male TRAMP mice
5
6 112 and three age-matched C57BL/6 male mice following the kit's protocol. After extraction and purification,
7
8 113 the gDNA samples were electrophoresed on an agarose gel, and the OD ratios were measured to confirm
9
10 114 the purity and concentrations of the gDNA prior to fragmentation by Covaris (Covaris, Inc., Woburn, MA
11
12 115 USA). The fragmented gDNA was then evaluated for size distribution and concentration using an Agilent
13
14 116 Bioanalyzer 2100 and a NanoDrop spectrophotometer.
15
16 117
17
18 118 **MeDIP-seq measurement**
19
20
21
22 119 Following the manufacturer's instructions, MeDIP was performed to analyze genome-wide
23
24 120 methylation using the MagMeDIP Kit from Diagenode (Diagenode Inc., Denville, NJ, USA). Methylated
25
26 121 DNA was separated from unmethylated fragments by immunoprecipitation with a 5-methylcytidine
27
28 122 monoclonal antibody from Eurogentec (Eurogentec S.A., Seraing, Belgium). Illumina libraries were then
29
30 123 created from the captured gDNA using NEBNext reagents (New England Biolabs, Ipswich, MA, USA).
31
32 124 Enriched libraries were evaluated for size distribution and concentration using an Agilent Bioanalyzer
33
34 125 2100, and the samples were then sequenced on an Illumina HiSeq2000 machine, which generated paired-
35
36 126 end reads of 90 or 100 nucleotides (nt). The results were analyzed for data quality and exome coverage
37
38 127 using the platform provided by DNAnexus (DNAnexus, Inc., Mountain View, CA, USA). The samples
39
40 128 were sent to Otogenetics Corp. (Norcross, GA) for Illumina sequencing and alignment with the reference
41
42 129 mouse genome. The resulting BAM files were downloaded for analysis.
43
44
45
46 130 Modified from the Trapnell method, the MeDIP alignments were compared with control sample
47
48 131 alignments using Cuffdiff 2.0.2 with no length correction [26]. A list of overlapping regions of sequence
49
50 132 alignment that were common to both the immunoprecipitated and control samples was created and used to
51
52 133 determine the quantitative enrichment of the MeDIP samples over the control samples using Cuffdiff;
53
54 134 statistically significant peaks (reads) at a 5% false discovery rate (FDR) and a minimum 4-fold difference,
55
56 135 as calculated using the Cummerbund package in R, were selected (Trapnell et al., 2012). Sequencing
57
58
59
60
61
62
63
64
65

1
2
3
4 136 reads were matched with the adjacent annotated genes using ChIPpeakAnno [27], and the uniquely
5 mapped reads were used to compare the differences between TRAMP and wild-type mice.
6
7

8
9 138 The reads were visualized and individual genes examined using Integrative Genomics Viewer
10 (IGV) [28]. IGV allows users to explore aligned reads at any level of details by changing resolution,
11 139 scrolling through and searching for specific chromosomes, genes or regions [29]. We specifically
12 140 examined genes that produced differences in methylation between the TRAMP and control groups of 4-
13 141 fold or more (Log_2 difference ≥ 2). IGV provided more in-depth understanding of these differences by
14 142 graphing distributions of reads against the reference genome. Heat maps were used to graphically
15 143 represent methylation levels in genes and to compare the methylation of the two groups. We used green
16 144 color to signify positive differences in methylation and the red color for the negative differences (TRAMP
17 145 minus control). Brighter shades correspond to more extreme values, i.e. larger fold-changes.
18
19
20
21
22
23
24
25
26
27
28
29 147
30
31 148 **Canonical pathways, diseases & function and network analysis by IPA**
32
33 149 Genes selected from the MeDIP-seq experiment based on significantly increased or decreased
34 fold changes (\log_2 -fold change ≥ 2) in the methylation pattern were analyzed (based on the p-values;
35 150 TRAMP vs. control) using IPA 4.0 (IPA 4.0, Ingenuity Systems, www.ingenuity.com),
36
37 151 the pathway enrichment p-value is calculated using the right-tailed Fisher Exact Test. A smaller p-value
38 indicated that the association was less likely to be random and more likely to be significant. In general,
39 152 values of 0.05 (for p-value) or 1.30 (for $-\log_{10}P$) were set as the thresholds. P-values less than 0.05 or –
40 153 $\log_{10}P$ more than 1.30 were considered to be statistically significant, non-random associations. IPA
41
42 154 utilized gene symbols to identify neighboring enriched methylation peaks using ChIPpeakAnno for all of
43
44 155 the analyses. Using IPA, 2147 genes from TRAMP group that showed a \log_2 -fold change ≥ 2 compared
45
46 156 with the control group were mapped. Based on these fold changes, IPA identified the canonical pathways,
47
48 157 biological functions/related diseases and networks that were closely related to the TRAMP model.
49
50
51 158
52
53 159
54
55
56 160
57
58
59
60 161 **MeDIP-seq data validation via Methylation-specific PCR (MSP)**
61
62
63
64
65

1
2
3
4 162 Genomic DNA was extracted and purified from 6 prostate samples (3 from TRAMP mice and 3
5 from normal C57BL/6 mice) using the AllPrep DNA/RNA/Protein Mini Kit (Qiagen, Valencia, CA,
6 USA). Then five hundred nanograms genomic DNA **was underwent** bisulfite conversion with an EZ DNA
7 Methylation-Gold Kit (Zymo Research Corp., Orange, CA) following the kit's protocol as described
8 previously [30]. The converted DNA was amplified by PCR using EpiTaq HS DNA polymerase
9 (Clontech Laboratories Inc, Mountain View, CA 94043, USA). According to MeDIP-seq results, four
10 target genes (2 with increased methylation and 2 with decreased methylation), **Dynein Cytoplasmic 1**
11 **Intermediate Chain 1 (DYN1I1)**, **Solute Carrier Family 1 Member 4 (SLC1A4)**, **XRCC6-Binding**
12 **Protein 1 (Xrcc6bp1)** and **Transthyretin (TTR)**, were selected for MSP validation. The primers' sequences
13 for the methylated reactions (MF and MR) and for the unmethylated reactions (UF and UR) and band size
14 of products are listed in Table 1. By running agarose gel electrophoresis, the amplification product bands
15 were isolated and were semi-quantitated by densitometry using ImageJ (Version 1.48d; NIH, Bethesda,
16 Maryland, USA).

17
18
19
20 175
21
22
23
24
25
26
27
28
29
30
31 176 **Validation of selected gene expression by Quantitative Real-time RT-PCR**
32
33
34
35
36
37
38 177 Total RNA was extracted and purified from 6 prostate samples (three from TRAMP mice and
39 three from normal C57BL/6 mice) using the same kit above. cDNA was synthesized from total RNA
40 using a SuperScript III First-Strand Synthesis System (Invitrogen, Grand Island, NY) following the kit's
41 instruction. mRNA levels were determined using quantitative real-time PCR (qPCR). **Histamine N-**
42 **Methyltransferase (HNMT)**, **Dync1i1**, **SLC1A4**, **Crystallin Zeta (CRYZ)** and **TTR** were randomly
43 selected to compare mRNA expression among WT and TRAMP mice prostate samples. The primers'
44 sequences for HNMT, DYNC1I1, SLC1A4, CRYZ, TTR and β -Actin are listed in Table 2.
45
46
47
48
49
50
51
52
53
54
55
56
57
58 184
59
60
61
62
63
64
65 185 **Results**
186 **MeDIP-seq results comparison**

One of our main targets was to screen and reveal aberrantly methylated genes to discover the related functions and pathways that might mediate the development of prostate cancer. To accomplish this goal in an unbiased manner, the MeDIP-seq results were analyzed using IPA. The first objective was to compare the total number of molecules with altered methylation in prostate samples of TRAMP mice to that of normal mice. Prostate samples were collected from the TRAMP and C57BL/6 mice, gDNA was isolated, and whole-genome DNA methylation analysis was performed using the described MeDIP-seq method. The results were analyzed in a paired manner, comparing the prostate tissue samples for each model. For the control, 16 509 344 (80.8%) mapped and 3 921 684 (19.2%) unmapped reads, for a total of 20 431 028 reads, were obtained. For the TRAMP mice, 12 097 771 (82.3%) mapped reads and 2 609 269 (17.7%) unmapped reads, for a total of 14 707 040 reads, were obtained (Fig. 1A). After identification and mapping to the library, the identified methylated regions (peaks) of the given genes were compared between the TRAMP and control mice, and IPA was used to identify the genes with significantly altered methylation in the TRAMP mice compared with the controls ($p<0.05$ or $-\log_{10}P>1.30$, and \log_2 -fold change ≥ 2).

Genes were sorted in the order of differences in methylation. Genes with the change in methylation levels of 4-fold or more (both, positive and negative) were then used as an input to the IPA software. According to the IPA setting, the p -value for a given process annotation was calculated by considering (1) the number of focus genes that participated in the process and (2) the total number of genes that are known to be associated with that process in the selected reference set. The more focus genes that are involved, the more likely the association is not due to random chance, resulting in a more significant p -value (larger $-\log_{10}P$ -value). Altogether, 2147 genes between the two groups showed a significant change (\log_2 -fold change ≥ 2) in methylated peaks. Compared with the control, significantly decreased methylation of 1105 genes and significantly increased methylation of 1042 genes were observed in TRAMP (Fig. 1B). The top fifty genes with increased methylation (Table 3) or decreased methylation (Table 4) located in promoter region, gene body or downstream of the gene were highlighted according to the \log_2 -fold change, ranking from the largest to the smallest change and with significant

1
2
3
4 213 statistic difference ($p < 0.05$). We also plotted the top 100 decreased or increased (Log2-fold Change)
5
6 214 methylated genes comparing with TRAMP to WT in different regions by MeDIP analysis, ranked by
7
8 215 alphabet (Fig. 2).

9
10
11 216 Four genes of interest, DYNC1I1, SLC1A4, XRCC6BP1 and TTR were analyzed by IGV (Fig. 3),
12
13 217 which provides more in-depth understanding of these differences between TRAMP and control mice. The
14
15 218 IGV results are in accordance with the MeDIP-seq finding. In TRAMP mice, the methylation ratio of
16
17 219 DYNC1I1 and SLC1A4 were increased, whereas the methylation ratio of TTR and XRCC6BP1 were
18
19 220 decreased. The methylation results have been validated by MSP.

20
21
22 221 These results demonstrate a fundamental difference in the global pattern of gene methylation
23
24 222 between the TRAMP prostate tumor and control prostate tissue. The potential impact of this difference
25
26 223 was further assessed using IPA by analyzing the canonical pathways, diseases and functions, and
27
28 224 networks related to these methylation changes.

29
30
31 225
32
33 226 **MeDIP-seq data validation by MSP**

34
35 227 According to the MeDIP-seq results, four interesting genes, two with increased methylation
36
37 228 (TRAMP vs WT), DYNC1I1 and SLC1A4, and two with decreased methylation (TRAMP vs WT),
38
39 229 XRCC6BP1 and TTR were selected to carry out MSP to validate the MeDIP-seq data. MSP results
40
41 230 indicated a similar trend in agreement with the MeDIP-seq results.

42
43 231 The results showed, in Dync1i1 and Slc1a4 genes, the relative density of M-MSP (methylated
44
45 232 MSP) to that of U-MSP (unmethylated MSP) in TRAMP group were increased, which indicated that the
46
47 233 CpG sites of these genes were hypermethylated in TRAMP mice (Fig. 4). Similarly, in Xrcc6bp1 and
48
49 234 TTR, the relative density of M-MSP to that of U-MSP in TRAMP group was decreased, which indicated
50
51 235 that the CpG sites of these genes were hypomethylated in TRAMP mice (Fig. 4).

52
53 236
54
55 237 **qPCR Validation of selected gene expression**

When mRNA levels were measured by qPCR, the relative expression levels of CRYZ, DYNC1I1, HNMT, SLC1A4 and TTR in TRAMP group were 0.62, 1.90, 0.15, 0.15 and 9.05 fold compared with WT (Fig. 5). Among these, TTR expression was increased by 9.05-fold over WT, which agreed with results reported by Wang et al. that expression levels of TTR were significantly higher in Prostate cancer tissue than in normal and benign prostate hyperplasia tissue [31]. When comparing mRNA expression and Methylation validation results, reciprocal relationships were found in TTR in TRAMP, which indicated decreased methylation in promoter region but increased gene expression when comparing with WT. In contrast, DNA methylation in the gene body or downstream may or may not follow a reciprocal relationship with gene expression as described in the findings of Yi-Zhou Jiang et.al. [32]. It is expected that individual genes may be differentially affected by CpG methylation and that only global analysis would be expected to reveal overall patterns likely to emerge.

Canonical pathway, diseases & functions and network analyses by IPA

The 2147 genes with remarkable change in methylation (\log_2 -fold change ≥ 2) were analyzed using the IPA software package. When using IPA, canonical pathways, which are based on the literature and are generated prior to data input, are the default settings. These pathways do not change upon data input and have a directionality-linked list of interconnected nodes. By contrast, networks are generated *de novo* based upon input data, lack directionality and contain molecules that are involved in a variety of canonical pathways.

The genes within the canonical pathways were ranked by the possibility parameter, i.e., the $-\log_{10}(P)$ value in the corresponding pathway, and are presented in Table 5. The CREB1 gene, which is involved the neuropathic pain signaling pathway, was ranked first. The top networks ranked based on their ratios of methylated gene/total gene are listed in Table 6. Of the networks, HDAC2-related, tissue morphology, embryonic development, and organ development network was ranked first (Table 6).

Among the networks, the cancer-related networks accounted for the majority (15/25) (Table 6), which

1
2
3
4 263 indicates that the great difference between the TRAMP and control lies in organ development and cancer
5
6 264 development.
7

8 265 Diseases & functions refer to the most likely linked diseases or functions based on statistics.
9
10
11 266 Similar to the network analysis, for the most associated disease based on the ranking of $-\log_{10}P$, cancer,
12
13 267 gastrointestinal disease, organismal abnormalities, reproductive system disease and dermatological
14
15 268 diseases were ranked within the top 5 (Fig. 6A). Of all cancer subtypes, adenocarcinoma ranked first (Fig.
16
17 269 6B), which was consistent with the TRAMP model, which is a model for prostate adenocarcinoma.
18
19
20 270
21

22 271 Discussion 23

24 272 **Analysis of canonical pathway would provide further understanding of disease and information for
25
26 the development of new therapeutic targets.**
27

28 274 As shown in Fig. 7, the genes with significantly altered methylation in the top canonical pathway
29
30 275 was the neuropathic pain signaling pathway, as mapped by IPA. This finding is consistent with
31
32 276 Chiaverotti's finding indicating that the most common malignancy in TRAMP is of neuroendocrine origin
33
34 277 [33]. Table 7 lists the genes involved in this pathway that exhibited modified methylation. Among these,
35
36 278 methylation of the CREB1 gene was found to be decreased by 2.274-fold (log2) by MeDIP-seq in
37
38 279 TRAMP.
40
41

42 280 CREB was first found to be closely related to cellular proliferation, differentiation and adaptive
43
44 281 responses in the neuronal system [34, 35]. Subsequently, increasing evidence revealed that CREB is
45
46 282 directly involved in the oncogenesis of a variety of cancers by regulating the immortalization and
47
48 283 transformation of cancer cells [36, 37].
50

51 284 CREB is also found to modulate other carcinogenesis pathways. **S100 Calcium Binding Protein P**
52
53 285 (S100P) is a calcium-binding protein that is associated with cancer, and functional analysis of the S100P
54
55 286 promoter identified SMAD, **signal transducer and activator of transcription (STAT)** /CREB and SP/KLF
56
57 287 binding sites as key regulatory elements in the transcriptional activation of the S100P gene in cancer
58
59 288 cells[38]. *Homo sapiens* lactate dehydrogenase c (hLdhc) was reported to be expressed in a wide
60
61
62
63
64
65

1
2
3
4 289 spectrum of tumors, including prostate cancers, and this expression was shown to be regulated by
5 transcription factor Sp1 and CREB as well as promoter CpG island (CGI) methylation [39, 40].
6
7 290 Decreased prostate tumorigenicity was found to be correlated with decreased expression of CREB and its
8 targets, including Bcl-2 and cyclin A1.
9
10
11
12

13 293 Clinically, upregulation of CREB was found in various human cancer samples including prostate
14 cancer, breast cancer, non-small-cell lung cancer and acute leukemia, whereas down-regulation of this
15 294 gene manifested inhibition of some cancer cells [41].
16
17
18
19

20 296 All of these data indicate that CREB is highly associated with cancer therapy. Our study
21 demonstrated that CREB gene methylation is significantly decreased in the TRAMP model, which
22 297 suggests a new approach to prostate cancer prevention and therapy.
23
24
25
26
27
28 300 **Novel networks involving the methylation of target genes could provide new insights for prostate**
29
30 301 **cancer.**

31
32 302 Compared with the canonical pathways, networks are generated *de novo* based upon input data
33 and are able to more flexibly reveal the interactions of altered genes and functions. As it is impossible to
34 303 analyze all networks listed in Table 6, four interesting networks were elaborated below (the higher the
35
36 304 score is, the more genes with altered methylation are involved in the network). Among all these networks,
37
38 305 many genes are known to be highly associated with tumor onset and progression, however, our insight
39
40 306 into their methylation status alteration would reveal novel biomarkers for prostate tumorigenesis.
41
42
43 307
44

45 308 **HDAC2-related network (Score=38):** The top network identified by IPA, was the HDAC2-related
46 tissue morphology, embryonic development and organ development network (Table 6, Fig. 8A). In this
47 309 network, the HDAC2 gene, a key member of HDAC, exhibited 3.274-fold (log2) decreased methylation
48
49 310 in TRAMP. HDACs are responsible for the removal of acetyl groups from histones and play important
50
51 311 roles in modulating the epigenetic process by influencing the expression of genes encoded by DNA bound
52
53 312 to a histone molecule [42]. HDAC inhibitors have also been shown to reduce colonic inflammation [43],
54
55 313 inhibit cell proliferation, and stimulate apoptosis, and these inhibitors represent a novel class of
56
57 314
58
59
60
61
62
63
64
65

therapeutic agents with antitumor activity that are currently in clinical development [44, 45]. By upregulating histone H3 acetylation and p21 gene expression, long-term treatment with MS-275, an HDAC inhibitor, attenuated the progression of prostate cancer *in vitro* and *in vivo* [46]. Another HDAC inhibitor, OSU-HDAC42, also showed a chemoprevention effect on prostate tumor progression in the TRAMP model [47]. Our data suggest that the altered methylation of HDAC (3.274 Log2-fold decrease) might be a novel, interesting target for prostate cancer treatment. Based on our MeDIP-seq results, HNMT in this network was increased by 3.703-fold (Log2). In addition, based on our qPCR analysis, HNMT gene expression was reduced by 6.67-fold, which supports the likelihood of a role of HNMT in prostate cancer. However, although HNMT has been demonstrated to be associated with breast cancer [48] and liver cancer [49], little is known about its potential role in prostate cancer, making it another potential novel marker.

GSTP1-related network (Score=16): GSTP1 expression is inactivated in prostate cancers [50-52], and this inactivation is associated with hypermethylation of GSTP1 CpG islands [51, 52]. Clinically, higher GSTP1 promoter methylation was found to be independently associated with the risk of prostate cancer [53]; therefore, the detection of hypermethylated GSTP1 in urine and semen samples can be a diagnostic marker of prostate cancer [54]. We also found that methylation of GSTP1 was an important factor involved in prostate cancer development. Interestingly, based on our data, the methylation of the GSTP1 gene was decreased 2.274-fold (log2) in TRAMP. Fig. 8B demonstrates the decreased methylation of GSTP1. Based on comparisons of prostate samples from TRAMP and strain-matched WT mice, Mavis CK et al. showed that promoter DNA hypermethylation does not appear to drive GST gene repression in TRAMP primary tumors [20]. The above results support our finding that the methylation status of GSTP1 may differ in humans. DYNC1I1, which was also in the network, exhibited a 4.926-fold (Log2) increase in methylation. In qPCR analysis, it indicates a 1.9-fold increase in gene expression. Although DYNC1I1 is significantly up-regulated in liver tumors [55] but not in prostate tumors, our findings suggest that it may be the next useful prostate cancer biomarker.

UBC-related network (Score=16): Another interesting network was found surrounding the UBC

1
2
3
4 341 gene (Fig. 8C); however, UBC itself was not identified by MeDIP-seq. The methylation of solute carrier
5 family 1 member 4 (SLC1A4) and CRYZ was highly up-regulated (3.807 and 3.703 Log2-fold increased,
6 respectively). According to qPCR results, the expressions of SLC1A4 and CRYZ in TRAMP group were
7 only 0.15 and 0.62 fold of WT group. SLC1A4 was found to be associated with human hepatocellular
8 carcinoma [56], and CRYZ was proven to be involved in **B-cell lymphoma 2 (BCL-2)** overexpression in
9 T-cell acute lymphocytic leukemia [57]. Although an association with prostate cancer was not found, our
10 344 MeDIP-seq findings in the TRAMP model suggest that this association is possible.
11
12
13
14
15
16
17
18
19
20 348 Merged networks overlaid with IPA settings could even predict the direction of the relationship.
21
22 349 When merging the two interesting networks HDAC2 and GSTP1 and overlaying the molecular activity
23 predictor of IPA (Fig. 9), tumor protein 53 (TP53) was found to be located in the center of the novel
24 350 network, indicating the potential important modulating function of TP53 on HDAC2 and GSTP1. TP53 is
25
26 351 encoded by p53, a tumor suppressor gene located on chromosome 17p13, which is one of the most
27 frequently mutated genes in multiple cancers [58-60]. TP53 acts as a transcription factor that mediates the
28 response to various cellular stresses, most importantly, the DNA damage response [61]. TP53 has also
29 353 been proven to play a crucial role in prostate cancer development and progression [62-64].
30
31
32
33
34
35
36
37
38 356 The interactions between GSTP1, HDAC and TP53 have been studied in prostate disease models.
39
40 357 In prostatectomy specimens of 30 benign prostatic hyperplasia patients, the increase in TP53 expression
41 at the same site was accompanied by an increase in GSTP1 expression [65]. In the 3 human prostate
42 358 cancer cell lines DU-145, PC-3 and LNCaP, As₂O₃ was found to increase TP53 expression only in
43
44 359 LNCap cells (without GSTP1 expression) but not in DU-145 and PC-3 cells (both cells expressed GSTP1)
45
46 360 [66]. In LNCaP cells, the acetylation of human TP53 increased the binding of promoter fragments of the
47
48 361 human P21 gene that contained a p53 response element and of the human HDAC2 protein [67].
49
50
51 362
52
53
54 363 Although the relationships between TP53 and HDAC2 as well as GSTP1 in prostate cancer have
55
56 364 been elucidated, these relationships in the TRAMP model remain unknown. Our predicated interactions
57
58 365 among these proteins in TRAMP suggest the possibility that TP53 influences the methylation of GSTP1
59
60 366 and HDAC2, which is a potential direction of future research.
61
62
63
64
65

1
2
3
4 367
5

6 368
7

Conclusions

8 369
9

10 370
11

12 371
13

14 372
15

16 373
17

18 374
19

20 375
21

22 376
23

24 377
25

26 378
27

29 379
30

32
33 380
34

35 381 **List of abbreviations:**
36

37 382 TRAMP-Transgenic adenocarcinoma of the mouse prostate
38

39 383 MeDIP - Methylated DNA immunoprecipitation
40

41 384 IPA- Ingenuity® pathway analysis
42

43 385 CREB1-Cyclic AMP (cAMP) response element-binding protein 1
44

45 386 HDAC2- Histone deacetyltransferase 2
46

47 387 GSTP1-Glutathione S-transferase 1
48

49 388 UBC- Polyubiquitin-C
50

51 389 NRF2-Nuclear factor (erythroid-derived 2)-like 2
52

53 390 MGMT-O6-alkylguanine DNA alkyltransferase
54

55 391 KLF6-Krueppel-like factor 6
56

57 392 DYNC1I1-Dynein Cytoplasmic 1 Intermediate Chain 1
58

59
60 393
61

62
63
64
65

To the best of our knowledge, this is the first MeDIP-seq study to analyze the DNA methylation differences of prostate cancer by comparing TRAMP mice, an adenocarcinoma prostate cancer model, with wild-type C57BL/6 mice. Cancer, especially adenocarcinoma, is the most commonly associated disease. MSP and qPCR have been used to validate the findings of MeDIP-seq. Using this MeDIP-seq and IPA analysis, comparisons between the TRAMP and control samples reveal profound differences in gene methylation. The analysis of canonical pathways and networks has identified important biological functions and molecular pathways that may mediate the development of adenocarcinoma prostate cancer. CREB-, HDAC2-, GSTP1- and UBC-related pathways showed significantly altered methylation profiles based on the canonical pathway and network analyses. Studies on epigenetics, such as DNA methylation, suggest novel avenues and strategies for the further development of biomarkers targeted for treatment and prevention approaches for prostate cancer.

TRAMP-Transgenic adenocarcinoma of the mouse prostate
MeDIP - Methylated DNA immunoprecipitation
IPA- Ingenuity® pathway analysis
CREB1-Cyclic AMP (cAMP) response element-binding protein 1
HDAC2- Histone deacetyltransferase 2
GSTM1-Glutathione S-transferase 1
UBC- Polyubiquitin-C
NRF2-Nuclear factor (erythroid-derived 2)-like 2
MGMT-O6-alkylguanine DNA alkyltransferase
KLF6-Krueppel-like factor 6
DYNC1I1-Dynein Cytoplasmic 1 Intermediate Chain 1

1
2
3
4 393 SLC1A4-Solute Carrier Family 1 Member 4
5
6 394 Xrcc6bp1-XRCC6-Binding Protein 1
7
8 395 TTR-Transthyretin
9
10 396 HNMT-Histamine N-Methyltransferase
11
12 397 CRYZ-Crystallin Zeta
13
14
15 398
16
17 399 **Acknowledgments**
18
19 400 The authors express sincere gratitude to all of the members of Dr. Tony Kong's laboratory for their
20 helpful discussions.
21
22 402
23
24
25 403 **Competing interests**
26
27 404 The authors declare that there are no competing interests.
28
29 405
30
31 406 **Authors' contributions**
32
33 407 Wenji Li designed the experiments. Wenji Li, Ying Huang and Davit Sargsyan performed the
34 experiments and acquired the data. All authors prepared the manuscript. All authors read and approved
35 the final manuscript.
36
37
38 410 **Contributor Information**
39
40 411 Wenji Li, Email: wl365@scarletmail.rutgers.edu.
41
42 412 Ying Huang, Email: huangyingms@gmail.com
43
44 413 Davit Sargsyan, Email: sargdavid@gmail.com
45
46 414 Tin Oo Khor, Email: t2khor@gmail.com
47
48 415 Yue Guo, Email: guoyue1990@gmail.com
49
50 416 Limin Shu, Email: lmnnshu@gmail.com
51
52 417 Anne Yuqing Yang, Email: anney2011@gmail.com
53
54 418 Chengyue Zhang, Email: chengyue.zhang@gmail.com
55
56 419 Ximena Paredes-Gonzalez, Email: xiparedes@gmail.com
57
58
59
60
61
62
63
64
65

1
2
3
4 420 Michael Verzi, Email: Verzi@dls.rutgers.edu
5
6 421 Ronald P Hart, Email: rhart@rutgers.edu
7
8 422 Ah-Ng Tony Kong, Email: kongt@pharmacy.rutgers.edu
9
10
11 423
12
13 424 **Availability of data and materials**
14
15 425 The data is freely shared and available for other investigators who need to use them.
16
17 426
18
19 427 **Consent for publication**
20
21 428 Not applicable.
22
23
24 429 **Ethics approval and consent to participate**
25
26 430 Animal care and use in this study was performed in accordance with Rutgers University Institutional
27 431 Animal Care and Use Committee (IACUC) standards (Approval Number 01-016).
28
29 432 **Funding**
30
31 433 This work was supported in part by institutional funds and by R01-AT009152 from the National Center
32 434 for Complementary and Integrative Health (NCCIH).
33
34
35 435
36
37 436
38
39
40
41
42
43
44
45
46
47
48
49
50
51
52
53
54
55
56
57
58
59
60
61
62
63
64
65

1
2
3
4 437 Table Legends
5
6 438
7
8 439 Table 1 Primer sequences used in MSP
9
10 440
11
12 441 Table 2 Primer sequences used in qPCR
13
14
15 442
16
17 443 Table 3 Top 50 annotated genes with increased methylation, ranked by log₂-fold change
18
19 444
20
21 445 Table 4 Top 50 annotated genes with decreased methylation, ranked by log₂-fold change
22
23 446
24
25
26 447 Table 5 Top 10 altered canonical pathways, sorted by -log₁₀ (P) value via IPA
27
28 448
29
30 449 Table 6 Top networks analyzed by IPA
31
32 450
33
34 451 Table 7 Altered methylation genes mapped to the neuropathic pain signaling pathway by IPA
35
36 452
37
38 453
39
40
41 454
42
43 455
44
45 456
46
47 457
48
49
50 458
51
52 459
53
54 460
55
56 461
57
58 462
59
60
61
62
63
64
65

1
2
3
4 463 Figure Legends
5
6 464 Fig. 1: Total mapping reads in the control and TRAMP mice (A) and the total number of significantly
7 (log₂-fold change ≥ 2) increased and decreased methylated genes in the TRAMP mice compared with the
8 control mice (B)
9
10
11 467 Fig. 2: Heat-map of Top 100 decreased or increased (Log₂-fold Change) methylated genes comparing
12 with TRAMP to WT in different regions by MeDIP analysis, ranked by alphabetic.
13
14
15 469 Fig. 3: Integrative Genomics Viewer visualization of the aligned reads' distribution against reference
16 genome for four targeted genes: DYNC1I1, SLC1A4, TTR and XRCC6BP1.
17
18
19 471 Fig. 4: Medip-Seq Validation by methylation-specific PCR (MSP). Representative electrophoretogram is
20 presented in the top panel. M-MSP: methylated reaction of MSP, U-MSP: unmethylated reaction of MSP.
21 The relative intensity of the methylated and unmethylated band was measured by ImageJ and presented in
22 the bottom panel. All of the data are presented as the mean \pm SD. **p* < 0.05 versus the control WT group.
23
24
25 475 Fig. 5: Comparison of mRNA expression of CRYZ, DYNC1I1, HNMT, SLC1A4 and TTR among WT
26 and TRAMP mice prostate samples. Total mRNA was isolated and analyzed using quantitative real-time
27 PCR. The data are presented as the mean \pm SD of three independent experiments. **p* < 0.05 versus the
28 control WT group.
29
30 479 Fig. 6: Top 5 associated disease categories (A) and top 5 cancer subtypes (B) analyzed by IPA
31
32
33 480 Fig. 7: Genes mapped to the canonical neuropathic pain signaling pathway by IPA. Red, increased
34 methylation; green, decreased methylation (for interpretation of the references to color in the figure
35 legend, please refer to the online version of this article)
36
37
38 483 Fig. 8: HDAC2 network (Score=38) (A), GSTP1 network (Score=16) (B), and UBC network (Score=16)
39 (C), as determined by IPA. Red, increased methylation; green, decreased methylation (for interpretation
40 of the references to color in the figure legend, please refer to the online version of this article)
41
42
43 486 Fig. 9: Merged network of the HDAC2 and GSTP1 networks, as determined by IPA. Red, increased
44 methylation; green, decreased methylation (for interpretation of the references to color in the figure
45 legend, please refer to the online version of this article)
46
47
48
49 490 **References**
50
51
52 491 1. Ferlay J, Shin HR, Bray F, Forman D, Mathers C, Parkin DM: **Estimates of worldwide burden of**
53 **cancer in 2008: GLOBOCAN 2008.** *International journal of cancer* 2010, **127**:2893-2917.
54
55 2. **United States Cancer Statistics: 1999–2011 Incidence and Mortality Web-based Report.**
56 [\[http://apps.cdc.gov/uscs/\]](http://apps.cdc.gov/uscs/)
57
58 3. Barbieri CE, Bangma CH, Bjartell A, Catto JW, Culig Z, Gronberg H, Luo J, Visakorpi T, Rubin MA:
59 **The mutational landscape of prostate cancer.** *Eur Urol* 2013, **64**:567-576.
60
61
62
63
64
65

- 1
2
3
4 497 4. Cuzick J, Thorat MA, Andriole G, Brawley OW, Brown PH, Culig Z, Eeles RA, Ford LG, Hamdy FC,
5 498 Holmberg L, et al: **Prevention and early detection of prostate cancer.** *Lancet Oncol* 2014,
6 499 **15**:e484-e492.
7
8 500 5. Strand SH, Orntoft TF, Sorensen KD: **Prognostic DNA Methylation Markers for Prostate Cancer.**
9 501 *Int J Mol Sci* 2014, **15**:16544-16576.
10 502 6. Matei DE, Nephew KP: **Epigenetic therapies for chemoresensitization of epithelial ovarian**
11 503 **cancer.** *Gynecol Oncol* 2010, **116**:195-201.
12 504 7. Jeong M, Goodell MA: **New answers to old questions from genome-wide maps of DNA**
13 505 **methylation in hematopoietic cells.** *Exp Hematol* 2014, **42**:609-617.
14 506 8. Ushijima T, Watanabe N, Okochi E, Kaneda A, Sugimura T, Miyamoto K: **Fidelity of the**
15 507 **methylation pattern and its variation in the genome.** *Genome Res* 2003, **13**:868-874.
16 508 9. Gama-Sosa MA, Slagel VA, Trewyn RW, Oxenhander R, Kuo KC, Gehrke CW, Ehrlich M: **The 5-**
17 509 **methylcytosine content of DNA from human tumors.** *Nucleic Acids Res* 1983, **11**:6883-6894.
18 510 10. Brothman AR, Swanson G, Maxwell TM, Cui J, Murphy KJ, Herrick J, Speights VO, Isaac J, Rohr LR:
19 511 **Global hypomethylation is common in prostate cancer cells: a quantitative predictor for**
20 512 **clinical outcome?** *Cancer Genet Cytogenet* 2005, **156**:31-36.
21 513 11. Seifert HH, Schmiemann V, Mueller M, Kazimirek M, Onofre F, Neuhausen A, Florl AR,
22 514 Ackermann R, Boecking A, Schulz WA, Grote HJ: **In situ detection of global DNA**
23 515 **hypomethylation in exfoliative urine cytology of patients with suspected bladder cancer.** *Exp*
24 516 *Mol Pathol* 2007, **82**:292-297.
25 517 12. Issa JP: **CpG island methylator phenotype in cancer.** *Nat Rev Cancer* 2004, **4**:988-993.
26 518 13. Shaw RJ, Hall GL, Lowe D, Bowers NL, Liloglou T, Field JK, Woolgar JA, Risk JM: **CpG island**
27 519 **methylation phenotype (CIMP) in oral cancer: associated with a marked inflammatory**
28 520 **response and less aggressive tumour biology.** *Oral Oncol* 2007, **43**:878-886.
29 521 14. Nazemalhosseini Mojarrad E, Kuppen PJ, Aghdaei HA, Zali MR: **The CpG island methylator**
30 522 **phenotype (CIMP) in colorectal cancer.** *Gastroenterol Hepatol Bed Bench* 2013, **6**:120-128.
31 523 15. Berg M, Hagland HR, Soreide K: **Comparison of CpG island methylator phenotype (CIMP)**
32 524 **frequency in colon cancer using different probe- and gene-specific scoring alternatives on**
33 525 **recommended multi-gene panels.** *PLoS One* 2014, **9**:e86657.
34 526 16. Hurwitz AA, Foster BA, Allison JP, Greenberg NM, Kwon ED: **The TRAMP mouse as a model for**
35 527 **prostate cancer.** *Curr Protoc Immunol* 2001, **Chapter 20**:Unit 20 25.
36 528 17. Valkenburg KC, Williams BO: **Mouse models of prostate cancer.** *Prostate Cancer* 2011,
37 529 **2011**:895238.
38 530 18. Yu S, Khor TO, Cheung KL, Li W, Wu TY, Huang Y, Foster BA, Kan YW, Kong AN: **Nrf2 expression is**
39 531 **regulated by epigenetic mechanisms in prostate cancer of TRAMP mice.** *PLoS One* 2010,
40 532 **5**:e8579.
41 533 19. McCabe MT, Low JA, Daignault S, Imperiale MJ, Wojno KJ, Day ML: **Inhibition of DNA**
42 534 **methyltransferase activity prevents tumorigenesis in a mouse model of prostate cancer.**
43 535 *Cancer Res* 2006, **66**:385-392.
44 536 20. Mavis CK, Morey Kinney SR, Foster BA, Karpf AR: **Expression level and DNA methylation status**
45 537 **of glutathione-S-transferase genes in normal murine prostate and TRAMP tumors.** *Prostate*
46 538 2009, **69**:1312-1324.
47 539 21. Pulukuri SM, Rao JS: **CpG island promoter methylation and silencing of 14-3-3sigma gene**
48 540 **expression in LNCaP and Tramp-C1 prostate cancer cell lines is associated with methyl-CpG-**
49 541 **binding protein MBD2.** *Oncogene* 2006, **25**:4559-4572.
50 542 22. Chiam K, Ryan NK, Ricciardelli C, Day TK, Buchanan G, Ochnik AM, Murti K, Selth LA, Australian
51 543 Prostate Cancer B, Butler LM, et al: **Characterization of the prostate cancer susceptibility gene**
52 544 **KLF6 in human and mouse prostate cancers.** *Prostate* 2013, **73**:182-193.
53
54
55
56
57
58
59
60
61
62
63
64
65

- 1
2
3
4 545 23. Morey Kinney SR, Zhang W, Pascual M, Greally JM, Gillard BM, Karasik E, Foster BA, Karpf AR:
5 546 **Lack of evidence for green tea polyphenols as DNA methylation inhibitors in murine prostate.**
6 547 *Cancer Prev Res (Phila)* 2009, **2**:1065-1075.
7
8 548 24. Wu TY, Khor TO, Su ZY, Saw CL, Shu L, Cheung KL, Huang Y, Yu S, Kong AN: **Epigenetic**
9 549 **modifications of Nrf2 by 3,3'-diindolylmethane in vitro in TRAMP C1 cell line and in vivo**
10 550 **TRAMP prostate tumors.** *AAPS J* 2013, **15**:864-874.
11 551 25. Khor TO, Yu S, Barve A, Hao X, Hong JL, Lin W, Foster B, Huang MT, Newmark HL, Kong AN:
12 552 **Dietary feeding of dibenzoylmethane inhibits prostate cancer in transgenic adenocarcinoma of**
13 553 **the mouse prostate model.** *Cancer Res* 2009, **69**:7096-7102.
14
15 554 26. Trapnell C, Roberts A, Goff L, Pertea G, Kim D, Kelley DR, Pimentel H, Salzberg SL, Rinn JL,
16 555 Pachter L: **Differential gene and transcript expression analysis of RNA-seq experiments with**
17 556 **TopHat and Cufflinks.** *Nat Protoc* 2012, **7**:562-578.
18
19 557 27. Zhu LJ, Gazin C, Lawson ND, Pages H, Lin SM, Lapointe DS, Green MR: **ChIPpeakAnno: a**
20 558 **Bioconductor package to annotate ChIP-seq and ChIP-chip data.** *BMC Bioinformatics* 2010,
21 559 **11**:237.
22
23 560 28. Thorvaldsdottir H, Robinson JT, Mesirov JP: **Integrative Genomics Viewer (IGV): high-**
24 561 **performance genomics data visualization and exploration.** *Brief Bioinform* 2013, **14**:178-192.
25
26 562 29. Robinson JT, Thorvaldsdottir H, Winckler W, Guttman M, Lander ES, Getz G, Mesirov JP:
27 563 **Integrative genomics viewer.** *Nat Biotechnol* 2011, **29**:24-26.
28
29 564 30. Khor TO, Huang Y, Wu TY, Shu L, Lee J, Kong AN: **Pharmacodynamics of curcumin as DNA**
30 565 **hypomethylation agent in restoring the expression of Nrf2 via promoter CpGs demethylation.**
31 566 *Biochem Pharmacol* 2011, **82**:1073-1078.
32
33 567 31. Wang D, Liang H, Mao X, Liu W, Li M, Qiu S: **Changes of transthyretin and clusterin after**
34 568 **androgen ablation therapy and correlation with prostate cancer malignancy.** *Transl Oncol* 2012,
35 569 **5**:124-132.
36
37 570 32. Jiang YZ, Manduchi E, Stoeckert CJ, Jr., Davies PF: **Arterial endothelial methylome: differential**
38 571 **DNA methylation in athero-susceptible disturbed flow regions in vivo.** *BMC Genomics* 2015,
39 572 **16**:506.
40
41 573 33. Chiaverotti T, Couto SS, Donjacour A, Mao JH, Nagase H, Cardiff RD, Cunha GR, Balmain A:
42 574 **Dissociation of epithelial and neuroendocrine carcinoma lineages in the transgenic**
43 575 **adenocarcinoma of mouse prostate model of prostate cancer.** *Am J Pathol* 2008, **172**:236-246.
44
45 576 34. Mayr B, Montminy M: **Transcriptional regulation by the phosphorylation-dependent factor**
46 577 **CREB.** *Nat Rev Mol Cell Biol* 2001, **2**:599-609.
47
48 578 35. Shaywitz AJ, Greenberg ME: **CREB: a stimulus-induced transcription factor activated by a**
49 579 **diverse array of extracellular signals.** *Annu Rev Biochem* 1999, **68**:821-861.
50
51 580 36. Sakamoto KM, Frank DA: **CREB in the pathophysiology of cancer: implications for targeting**
52 581 **transcription factors for cancer therapy.** *Clin Cancer Res* 2009, **15**:2583-2587.
53
54 582 37. Conkright MD, Montminy M: **CREB: the unindicted cancer co-conspirator.** *Trends Cell Biol* 2005,
55 583 **15**:457-459.
56
57 584 38. Gibadulinova A, Tothova V, Pastorek J, Pastorekova S: **Transcriptional regulation and functional**
58 585 **implication of S100P in cancer.** *Amino Acids* 2011, **41**:885-892.
59
60 586 39. Tang H, Goldberg E: **Homo sapiens lactate dehydrogenase c (Ldhc) gene expression in cancer**
61 587 **cells is regulated by transcription factor Sp1, CREB, and CpG island methylation.** *J Androl* 2009,
62 588 **30**:157-167.
63
64 589 40. Park MH, Lee HS, Lee CS, You ST, Kim DJ, Park BH, Kang MJ, Heo WD, Shin EY, Schwartz MA, Kim
65 590 EG: **p21-Activated kinase 4 promotes prostate cancer progression through CREB.** *Oncogene*
591 **2013, 32**:2475-2482.

- 1
2
3
4 592 41. Xiao X, Li BX, Mitton B, Ikeda A, Sakamoto KM: **Targeting CREB for cancer therapy: friend or foe.**
5 593 *Curr Cancer Drug Targets* 2010, **10**:384-391.
6 594 42. Bassett SA, Barnett MP: **The Role of Dietary Histone Deacetylases (HDACs) Inhibitors in Health**
7 595 **and Disease.** *Nutrients* 2014, **6**:4273-4301.
8 596 43. Glauben R, Batra A, Stroh T, Erben U, Fedke I, Lehr HA, Leoni F, Mascagni P, Dinarello CA, Zeitz M,
9 597 Siegmund B: **Histone deacetylases: novel targets for prevention of colitis-associated cancer in**
10 598 **mice.** *Gut* 2008, **57**:613-622.
11 599 44. Giannini G, Cabri W, Fattorusso C, Rodriguez M: **Histone deacetylase inhibitors in the**
12 600 **treatment of cancer: overview and perspectives.** *Future Med Chem* 2012, **4**:1439-1460.
13 601 45. Kim HJ, Bae SC: **Histone deacetylase inhibitors: molecular mechanisms of action and clinical**
14 602 **trials as anti-cancer drugs.** *Am J Transl Res* 2011, **3**:166-179.
15 603 46. Qian DZ, Wei YF, Wang X, Kato Y, Cheng L, Pili R: **Antitumor activity of the histone deacetylase**
16 604 **inhibitor MS-275 in prostate cancer models.** *Prostate* 2007, **67**:1182-1193.
17 605 47. Sargeant AM, Rengel RC, Kulp SK, Klein RD, Clinton SK, Wang YC, Chen CS: **OSU-HDAC42, a**
18 606 **histone deacetylase inhibitor, blocks prostate tumor progression in the transgenic**
19 607 **adenocarcinoma of the mouse prostate model.** *Cancer Res* 2008, **68**:3999-4009.
20 608 48. He GH, Lin JJ, Cai WK, Xu WM, Yu ZP, Yin SJ, Zhao CH, Xu GL: **Associations of polymorphisms in**
21 609 **histidine decarboxylase, histamine N-methyltransferase and histamine receptor H3 genes with**
22 610 **breast cancer.** *PLoS One* 2014, **9**:e97728.
23 611 49. Roh T, Kwak MY, Kwak EH, Kim DH, Han EY, Bae JY, Bang du Y, Lim DS, Ahn IY, Jang DE, et al:
24 612 **Chemopreventive mechanisms of methionine on inhibition of benzo(a)pyrene-DNA adducts**
25 613 **formation in human hepatocellular carcinoma HepG2 cells.** *Toxicol Lett* 2012, **208**:232-238.
26 614 50. Nelson WG, De Marzo AM, DeWeese TL, Isaacs WB: **The role of inflammation in the**
27 615 **pathogenesis of prostate cancer.** *J Urol* 2004, **172**:S6-11; discussion S11-12.
28 616 51. Lin X, Tascilar M, Lee WH, Vles WJ, Lee BH, Veeraswamy R, Asgari K, Freije D, van Rees B, Gage
29 617 WR, et al: **GSTP1 CpG island hypermethylation is responsible for the absence of GSTP1**
30 618 **expression in human prostate cancer cells.** *Am J Pathol* 2001, **159**:1815-1826.
31 619 52. Nelson CP, Kidd LC, Sauvageot J, Isaacs WB, De Marzo AM, Groopman JD, Nelson WG, Kensler
32 620 TW: **Protection against 2-hydroxyamino-1-methyl-6-phenylimidazo[4,5-b]pyridine cytotoxicity**
33 621 **and DNA adduct formation in human prostate by glutathione S-transferase P1.** *Cancer Res*
34 622 2001, **61**:103-109.
35 623 53. Maldonado L, Brait M, Loyo M, Sullenberger L, Wang K, Peskoe SB, Rosenbaum E, Howard R,
36 624 Toubaji A, Albadine R, et al: **GSTP1 promoter methylation is associated with recurrence in early**
37 625 **stage prostate cancer.** *J Urol* 2014, **192**:1542-1548.
38 626 54. Bryzgunova OE, Morozkin ES, Yarmoschuk SV, Vlassov VV, Laktionov PP: **Methylation-specific**
39 627 **sequencing of GSTP1 gene promoter in circulating/extracellular DNA from blood and urine of**
40 628 **healthy donors and prostate cancer patients.** *Ann NY Acad Sci* 2008, **1137**:222-225.
41 629 55. Dong H, Zhang H, Liang J, Yan H, Chen Y, Shen Y, Kong Y, Wang S, Zhao G, Jin W: **Digital**
42 630 **karyotyping reveals probable target genes at 7q21.3 locus in hepatocellular carcinoma.** *BMC*
43 631 **Med Genomics** 2011, **4**:60.
44 632 56. Marshall A, Lukk M, Kutter C, Davies S, Alexander G, Odom DT: **Global gene expression profiling**
45 633 **reveals SPINK1 as a potential hepatocellular carcinoma marker.** *PloS one* 2013, **8**:e59459.
46 634 57. Lapucci A, Lulli M, Amedei A, Papucci L, Witort E, Di Gesualdo F, Bertolini F, Brewer G, Nicolin A,
47 635 Bevilacqua A, et al: **zeta-Crystallin is a bcl-2 mRNA binding protein involved in bcl-2**
48 636 **overexpression in T-cell acute lymphocytic leukemia.** *FASEB J* 2010, **24**:1852-1865.
49 637 58. Wang X, Zhang X, He P, Fang Y: **Sensitive detection of p53 tumor suppressor gene using an**
50 638 **enzyme-based solid-state electrochemiluminescence sensing platform.** *Biosens Bioelectron*
51 639 2011, **26**:3608-3613.
52
53
54
55
56
57
58
59
60
61
62
63
64
65

- 1
2
3
4 640 59. Parkinson EK: **Senescence as a modulator of oral squamous cell carcinoma development.** *Oral*
5 641 *Oncol* 2010, **46**:840-853.
6 642 60. Hickman JA, Potten CS, Merritt AJ, Fisher TC: **Apoptosis and cancer chemotherapy.** *Philos Trans R Soc Lond B Biol Sci* 1994, **345**:319-325.
7 643
8 644 61. Rokavec M, Li H, Jiang L, Hermeking H: **The p53/microRNA connection in gastrointestinal**
9 645 **cancer.** *Clin Exp Gastroenterol* 2014, **7**:395-413.
10 646 62. Thomas P, Pang Y, Dong J, Berg AH: **Identification and Characterization of Membrane Androgen**
11 647 **Receptors in the ZIP9 Zinc Transporter Subfamily: II. Role of Human ZIP9 in Testosterone-**
12 648 **Induced Prostate and Breast Cancer Cell Apoptosis.** *Endocrinology* 2014, **155**:4250-4265.
13 649 63. Lin VC, Huang CY, Lee YC, Yu CC, Chang TY, Lu TL, Huang SP, Bao BY: **Genetic variations in TP53**
14 648 **binding sites are predictors of clinical outcomes in prostate cancer patients.** *Arch Toxicol* 2014,
15 649 **88**:901-911.
16 650
17 651
18 652 64. Antonarakis ES, Keizman D, Zhang Z, Gurel B, Lotan TL, Hicks JL, Fedor HL, Carducci MA, De
19 653 Marzo AM, Eisenberger MA: **An immunohistochemical signature comprising PTEN, MYC, and**
20 654 **Ki67 predicts progression in prostate cancer patients receiving adjuvant docetaxel after**
21 655 **prostatectomy.** *Cancer* 2012, **118**:6063-6071.
22 656 65. Wang W, Bergh A, Damber JE: **Increased p53 immunoreactivity in proliferative inflammatory**
23 657 **atrophy of prostate is related to focal acute inflammation.** *APMIS* 2009, **117**:185-195.
24 658 66. Lu M, Xia L, Luo D, Waxman S, Jing Y: **Dual effects of glutathione-S-transferase pi on As2O3**
25 659 **action in prostate cancer cells: enhancement of growth inhibition and inhibition of apoptosis.**
26 660 *Oncogene* 2004, **23**:3945-3952.
27 661 67. Roy S, Tenniswood M: **Site-specific acetylation of p53 directs selective transcription complex**
28 662 **assembly.** *J Biol Chem* 2007, **282**:4765-4771.
29 663
30
31
32
33
34
35
36
37
38
39
40
41
42
43
44
45
46
47
48
49
50
51
52
53
54
55
56
57
58
59
60
61
62
63
64
65

Table 1 Primer sequences used in MSP

Gene name	Primer name	Primer sequence	Band size (bp)
Dync1i1	Dync1i1-MF*	TATGAAGAAAAATATAAGATAACGG	232
	Dync1i1-MR*	ACGAACATTCACATTCGAA	
	Dync1i1-UF*	TTTATGAAGAAAAATATAAGATAATGG	235
	Dync1i1-UR*	CACAAACATTCACATTCAAA	
Slc1a4	Slc1a4-MF	ATAAATTATTTTTTATGTTACGG	216
	Slc1a4-MR	TTAATAATACATACCTATAATCCGAC	
	Slc1a4-UF	ATAAATTATTTTTTATGTTATGG	216
	Slc1a4-UR	TTAATAATACATACCTATAATCCAAC	
Xrcc6bp1	Xrcc6bp1-MF	GTAAATGTGAGAGTTAGAATAGTATAGGAC	110
	Xrcc6bp1-MR	AATTAATACAATATTCGATACCGAT	
	Xrcc6bp1-UF	GTAAATGTGAGAGTTAGAATAGTATAGGAT	110
	Xrcc6bp1-UR	AATTAATACAATATTCAAATACCAAT	
TTR	TTR-MF	GGAATTAAAGATAACGGTTATATCGA	106
	TTR-MR	AACACTCTTCGAACATACTCGAC	
	TTR-UF	AGGAATTAAAGATATGGTTATATTGA	108
	TTR-UR	AAACACTCTTCAAACATACTCAAC	

*:-MF: forward primer sequence for the methylated reactions; -MR: reverse primer sequence for the unmethylated reactions;-UF: forward primer sequence for the unmethylated reactions; -UR: reverse primer sequence for the unmethylated reactions. Primer sequences are started from 5' (left) to 3' (right).

Table 2 Primer sequences used in qPCR

Gene name	Primer name	Primer sequence
HNMT	sense	5' -GCTGCCAGTGCTAAAATTCTC -3'
	antisense	5' -CAGGTCATCCAGTATCTGCG -3'
DYNC1I1	sense	5' -GTGTACGATGTCATGTGGTCC-3'
	antisense	5' -AACTCGGTTAG GGCAGATG-3'
SLC1A4	sense	5' -CCTCACATTGCCATCATCTT G-3'
	antisense	5' -CATCCCCTCCACATTCAACC-3'
CRYZ	sense	5' -GCAGCCGATGACACTATCTAC-3'
	antisense	5' -GCCCATGAACCAAAACG -3'
TTR	sense	5' -AATCGTACTGGAAGACACTTGG-3'
	antisense	5' -TGGTGCTGTAGGAGTATGGG -3'
β-Actin	sense	5' -CGTTCAATACCCCAGCCATG-3'
	antisense	5' -ACCCCGTCACCAGAGTCC-3'

Table 3 Top 50 annotated genes with increased methylation, ranked by log₂-fold change

Rank	Symbol	Gene Name	Log ₂ -fold Change	Location	Type(s)	Methylation Region
(TRAMP/WT)						
1	FGD4	FYVE, RhoGEF and PH domain containing 4	4.993	Cytoplasm	other	promoter
2	MED13L	mediator complex subunit 13-like	4.993	Nucleus	other	downstream
3	DYNC1I1	dynein, cytoplasmic 1, intermediate chain 1	4.926	Cytoplasm	other	body
4	XK	X-linked Kx blood group	4.781	Plasma Membrane	transporter	body
5	EAPP	E2F-associated phosphoprotein	4.703	Cytoplasm	other	body
6	TGFA	transforming growth factor, alpha	4.534	Extracellular Space	growth factor	promoter
7	BTG1	B-cell translocation gene 1, anti-proliferative	4.440	Nucleus	transcription regulator	promoter
8	BARD1	BRCA1 associated RING domain 1	4.341	Nucleus	transcription regulator	promoter
9	GJA1	gap junction protein, alpha 1, 43 kDa	4.341	Plasma Membrane	transporter	promoter
10	Zfp640	zinc finger protein 640	4.234	Other	other	downstream
11	S100A5	S100 calcium-binding protein A5	4.119	Nucleus	other	promoter
12	SOX17	SRY (sex-determining region	4.119	Nucleus	transcription	downstream

		Y)-box 17			regulator	
13	PDGFRL	platelet-derived growth factor receptor-like	3.993	Plasma Membrane	kinase	body
14	ZKSCAN2	zinc finger with KRAB and SCAN domains 2	3.993	Nucleus	transcription regulator	promoter
15	DMXL2	Dmx-like 2	3.926	Cytoplasm	other	body
16	LEPR	leptin receptor	3.926	Plasma Membrane	transmembrane receptor	body
17	AOAH	acyloxyacyl hydrolase (neutrophil)	3.855	Extracellular Space	enzyme	promoter
18	Apol7e	apolipoprotein L 7e	3.855	Other	other	body
19	CACNG6	calcium channel, voltage-dependent, gamma subunit 6	3.855	Plasma Membrane	ion channel	promoter
20	CHCHD3	coiled-coil-helix-coiled-coil-helix domain containing 3	3.855	Cytoplasm	other	body
21	FAM174B	family with sequence similarity 174, member B	3.855	Other	other	body
22	GALNT13	polypeptide N-acetylgalactosaminyltransferase	3.855	Cytoplasm	enzyme	body
23	GPR37	G protein-coupled receptor 37 (endothelin receptor type B-like)	3.855	Plasma Membrane	G-protein coupled receptor	downstream
24	Mup1	major urinary protein 1	3.855	Extracellular Space	other	downstream

25	NGF	nerve growth factor (beta polypeptide)	3.855	Extracellular Space	growth factor	downstream
26	OLFM3	olfactomedin 3	3.855	Cytoplasm	other	body
27	PCBP3	poly(rC)-binding protein 3	3.855	Nucleus	other	body
28	RBMS3	RNA-binding motif, single-stranded-interacting protein 3	3.855	Other	other	body
29	TMX1	thioredoxin-related transmembrane protein 1	3.855	Cytoplasm	enzyme	downstream
30	ZNF14	zinc finger protein 14	3.855	Nucleus	transcription regulator	body
31	SLC1A4	solute carrier family 1 (glutamate/neutral amino acid transporter), member 4	3.807	Plasma Membrane	transporter	body
32	ZFAND3	zinc finger, AN1-type domain 3	3.717	Other	other	body
33	C1orf162	chromosome 1 open reading frame 162	3.703	Other	transporter	promoter
34	C9orf131	chromosome 9 open reading frame 131	3.703	Other	other	body
35	CRYZ	crystallin, zeta (quinone reductase)	3.703	Cytoplasm	enzyme	body
36	CYP2A6	cytochrome P450, family 2, subfamily A, polypeptide 6	3.703	Cytoplasm	enzyme	body
37	CYP51A1	cytochrome P450, family 51, subfamily A, polypeptide 1	3.703	Cytoplasm	enzyme	downstream
38	DSPP	dentin sialophosphoprotein	3.703	Extracellular	other	promoter

Space						
39	GALNT3	polypeptide N-acetylgalactosaminyltransferase 3	3.703	Cytoplasm	enzyme	downstream
40	Gm4836	predicted gene 4836	3.703	Nucleus	other	downstream
41	GRIP1	glutamate receptor-interacting protein 1	3.703	Plasma Membrane	transcription regulator	promoter
42	GUCY1A2	guanylate cyclase 1, soluble, alpha 2	3.703	Cytoplasm	enzyme	body
43	HNMT	histamine N-methyltransferase	3.703	Cytoplasm	enzyme	body
44	LRRC8B	Leucine-rich repeat containing 8 family, member B	3.703	Other	other	body
45	MEF2A	myocyte enhancer factor 2A	3.703	Nucleus	transcription regulator	body
46	NRG3	neuregulin 3	3.703	Extracellular Space	growth factor	promoter
47	PCDH17	protocadherin 17	3.703	Other	other	promoter
48	PDP2	pyruvate dehydrogenase phosphatase catalytic subunit 2	3.703	Cytoplasm	phosphatase	promoter
49	SH2D4B	SH2 domain containing 4B	3.703	Other	other	body
50	Smok2b	sperm motility kinase 2B	3.703	Other	kinase	body

Table 4 Top 50 annotated genes with decreased methylation, ranked by log₂-fold change

Ran k	Symbol	Gene Name	Log ₂ fold Change	Location	Type(s)	Methylatio n region
			(TRAMP/W T)			
1	Rrbp1	Ribosome-binding protein 1	-5.824	Cytoplasm	transporter	body
2	CISD2	CDGSH iron sulfur domain 2	-4.373	Cytoplasm	other	downstream
3	NR4A1	nuclear receptor subfamily 4, group A, member 1	-4.324	Nucleus	ligand- dependent nuclear receptor	body
4	LCMT1	leucine carboxyl methyltransferase 1	-4.051	Cytoplasm	enzyme	body
5	XRCC6BP 1	XRCC6 binding protein 1	-3.990	Other	kinase	downstream
6	TTR	transthyretin	-3.926	Extracellular Space	transporter	promoter
7	ZNF536	zinc finger protein 536	-3.859	Other	other	downstream
8	FARP1	FERM, RhoGEF (ARHGEF) and pleckstrin domain protein 1	-3.788	Plasma Membrane	other	body

(chondrocyte-

derived)

9	TNRC18	trinucleotide repeat containing 18	-3.788	Other	other	body
10	FOXL1	forkhead box L1	-3.714	Nucleus	transcription	downstream regulator
11	ZMAT4	zinc finger, matrin- type 4	-3.714	Nucleus	other	promoter
12	ABCC2	ATP-binding cassette, sub-family C (CFTR/MRP), member 2	-3.636	Plasma Membrane	transporter	body
13	AMFR	autocrine motility factor receptor, E3 ubiquitin protein ligase	-3.636	Plasma Membrane	transmembran e receptor	downstream
14	ARSK	arylsulfatase family, member K	-3.636	Extracellular Space	enzyme	body
15	GRM3	glutamate receptor, metabotropic 3	-3.636	Plasma Membrane	G-protein coupled receptor	promoter
16	HTR1F	5- hydroxytryptamine (serotonin) receptor 1F, G protein-	-3.636	Plasma Membrane	G-protein coupled receptor	body

		coupled				
17	CC2D2A	coiled-coil and C2 domain containing 2A	-3.554	Other	other	promoter
18	CSMD1	CUB and Sushi multiple domains 1	-3.554	Plasma	other	body
19	HIBCH	3-hydroxyisobutyryl-CoA hydrolase	-3.554	Cytoplasm	enzyme	body
20	NMT2	N-myristoyltransferase 2	-3.554	Cytoplasm	enzyme	promoter
21	PCDH20	protocadherin 20	-3.554	Other	other	promoter
22	PDCD1	programmed cell death 1	-3.554	Plasma	phosphatase	promoter
23	QRFP	pyroglutamylated RFamide peptide	-3.554	Extracellular Space	other	downstream
24	REG3G	regenerating islet-derived 3 gamma	-3.554	Extracellular Space	other	downstream
25	TLR4	toll-like receptor 4	-3.554	Plasma	transmembrane receptor	downstream
26	TNRC6B	trinucleotide repeat containing 6B	-3.554	Other	other	body
27	CCR3	chemokine (C-C motif) receptor 3	-3.466	Plasma	G-protein coupled	promoter

receptor						
28	Cngb1	cyclic nucleotide gated channel beta 1	-3.466	Other	other	body
29	CNTNAP5	contactin associated protein-like 5	-3.466	Other	other	body
30	Cox7c	cytochrome c oxidase subunit VIIc	-3.466	Cytoplasm	other	promoter
31	EIF4EBP1	eukaryotic translation initiation factor 4E binding protein 1	-3.466	Cytoplasm	translation regulator	downstream
32	FGF10	fibroblast growth factor 10	-3.466	Extracellular Space	growth factor	downstream
33	GNAI1	guanine nucleotide-binding protein (G protein), alpha inhibiting activity polypeptide 1	-3.466	Plasma Membrane	enzyme	promoter
34	Ins1	insulin I	-3.466	Extracellular Space	other	promoter
35	ITGA8	integrin, alpha 8	-3.466	Plasma Membrane	other	body
36	JAG1	jagged 1	-3.466	Extracellular Space	growth factor	promoter

37	Pcdh10	protocadherin 10	-3.466	Other	other	promoter
38	PPP1R17	protein phosphatase subunit 17, regulatory	-3.466	Cytoplasm	other	downstream
39	Serbp1	Serpine1 mRNA-binding protein 1	-3.466	Cytoplasm	other	promoter
40	Wasl	Wiskott-Aldrich syndrome-like (human)	-3.466	Cytoplasm	other	promoter
41	ABAT	4-aminobutyrate aminotransferase	-3.373	Cytoplasm	enzyme	body
42	ANKMY2	ankyrin repeat and MYND domain containing 2	-3.373	Plasma Membrane	other	downstream
43	Card11	caspase recruitment domain family, member 11	-3.373	Other	other	body
44	CDK5R1	cyclin-dependent kinase 5, regulatory subunit 1 (p35)	-3.373	Nucleus	kinase	downstream
45	DACH1	dachshund family transcription factor 1	-3.373	Nucleus	transcription regulator	downstream
46	FGGY	FGGY carbohydrate kinase domain	-3.373	Other	other	body

		containing					
47	GADD45G	growth arrest and DNA-damage- inducible, gamma	-3.373	Nucleus	other		downstream
48	GLRB	glycine receptor, beta	-3.373	Plasma	ion channel	body	
49	LRRTM1	Leucine-rich repeat transmembrane neuronal 1	-3.373	Plasma	other		downstream
50	NEDD4L	neural precursor cell expressed, developmentally down-regulated 4- like, E3 ubiquitin protein ligase	-3.373	Cytoplasm	enzyme	body	

Table 5 Top 10 altered canonical pathways, sorted by $-\log_{10}(P)$ value via IPA

Pathways	$-\log_{10}(p\text{-value})$	Involved Molecules
Neuropathic Pain	3.01	TACR1, GRM7, KCNN3, CAMK1D, MAPK1, GPR37, BDNF,
Signaling In Dorsal Horn Neurons		GRM3, GRIA1, CREB1, TAC1, GRIN3A
Cardiomyocyte Differentiation via BMP Receptors	3.01	NKX2-5, MAP3K7, SMAD6, MEF2C, BMP10
cAMP-mediated Signaling	2.75	ENPP6, ADCY2, RGS18, MAPK1, CAMK1D, PTGER3, GRM3, DUSP6, GNAI1, CHRM3, Cngb1, GRM7, FSHR, RGS10, CREB1, HTR1F, DRD3, PTGER4, PPP3CA
Estrogen Biosynthesis	2.64	CYP4F8, CYP3A5, HSD17B7, CYP2C9, CYP2A6 (includes others), CYP51A1, CYP2C8
PXR/RXR Activation	2.63	CYP3A5, ABCC2, INS, CYP2C9, CYP2A6 (includes others), INSR, PAPSS2, Ins1, CYP2C8
Wnt/β-catenin Signaling	2.43	CDKN2A, GJA1, WNT3, APPL2, APC, SOX17, SOX2, FZD8, PPP2R1A, WNT7A, RARB, TLE4, MAP3K7, NR5A2, GSK3B
BMP Signaling Pathway	2.43	MAP2K4, NKX2-5, MAPK1, BMP8A, CREB1, MAP3K7, SMAD6, GREM1, BMP10
Factors Promoting Cardiogenesis in Vertebrates	2.41	FZD8, SMAD2, NKX2-5, WNT3, BMP8A, MAP3K7, MEF2C, GSK3B, BMP10, APC
Glutamate	2.40	GRM7, SLC1A4, GRM3, GRIA1, SLC38A1, GRIP1, GRIK2,

Receptor Signaling	GRIN3A
Human Embryonic Stem Cell	2.39 SOX2, FZD8, SMAD2, WNT7A, WNT3, BDNF, BMP8A, SMAD6, GSK3B, NGF, APC, INHBA, BMP10
Pluripotency	
LPS/IL-1 Mediated	2.37 MAP2K4, GAL3ST2, ABCC2, CYP2C9, APOC2, NDST4, PAPSS2, IL1R2, TLR4, UST, CYP3A5, Sult1c2 (includes others), MAP3K7, NR5A2, CYP2A6 (includes others), GSTP1, MAOA, CYP2C8
Inhibition of RXR Function	

Table 6 Top networks analyzed by IPA

Rank	Top Diseases and Functions	Score
1	Tissue Morphology, Embryonic Development, Organ Development	38
2	Cell-To-Cell Signaling and Interaction, Cell Signaling, Cellular Function and Maintenance	38
3	Cell Death and Survival, Cancer, Cell Morphology	37
4	Cancer, Gastrointestinal Disease, Cell Death and Survival	35
5	Cancer, Carbohydrate Metabolism, Small Molecule Biochemistry	33
6	Cancer, Cell Death and Survival, Cellular Response to Therapeutics	33
7	Lymphoid Tissue Structure and Development, Organ Morphology, Organismal Development	30
8	Cancer, Gastrointestinal Disease, Post-Translational Modification	29
9	Cancer, Dermatological Diseases and Conditions, Gastrointestinal Disease	29
10	Cell Morphology, Digestive System Development and Function, Nervous System Development and Function	28
11	Cancer, Gastrointestinal Disease, Cell Death and Survival	26
12	Cancer, Drug Metabolism, Energy Production	26
13	Cell-To-Cell Signaling and Interaction, Nervous System Development and Function, Cellular Development	26
14	Cellular Movement, Cellular Development, Skeletal and Muscular System Development and Function	24
15	Cell Death and Survival, Cancer, Cellular Development	24
16	Hereditary Disorder, Inflammatory Response, Metabolic Disease	22

17	Cell Morphology, Nervous System Development and Function, Tissue Morphology	21
18	Cancer, Organismal Injury and Abnormalities, Reproductive System Disease	21
19	Cellular Compromise, Cancer, Cardiovascular Disease	19
20	Cell-To-Cell Signaling and Interaction, Tissue Development, Hematological System Development and Function	17
21	Cancer, Organismal Survival, Organismal Injury and Abnormalities	16
22	Cellular Assembly and Organization, Cellular Function and Maintenance, Embryonic Development	16
23	Cancer, Organismal Injury and Abnormalities, Reproductive System Disease	16
24	Cell Cycle, Cellular Movement, Cancer	16
25	Cancer, Developmental Disorder, Hereditary Disorder	16

Table 7

Altered methylation genes mapped to the neuropathic pain signaling pathway by IPA

Symbol	Gene Name	Log ₂ -Fold Change	Type(s)
GRM3	glutamate receptor, metabotropic 3	-3.636	G-protein-coupled receptor
GRIA1	glutamate receptor, ionotropic, AMPA 1	-3.167	ion channel
BDNF	brain-derived neurotrophic factor	-2.373	growth factor
CREB1	cAMP-responsive element-binding protein 1	-2.274	transcription regulator
GRM7	glutamate receptor, metabotropic 7	-2.274	G-protein-coupled receptor
GRIN3A	glutamate receptor, ionotropic, N-methyl-D-aspartate 3A	-2.129	ion channel
MAPK1	mitogen-activated protein kinase 1	2.048	kinase
TAC1	tachykinin, precursor 1	2.408	other
CAMK1	calcium/calmodulin-dependent protein kinase ID	2.855	kinase
D			
TACR1	tachykinin receptor 1	2.855	G-protein-coupled receptor
KCNN3	potassium intermediate/small conductance calcium-activated channel, subfamily N, member 3	3.119	ion channel
GPR37	G protein-coupled receptor 37 (endothelin receptor type B-like)	3.855	G-protein-coupled receptor

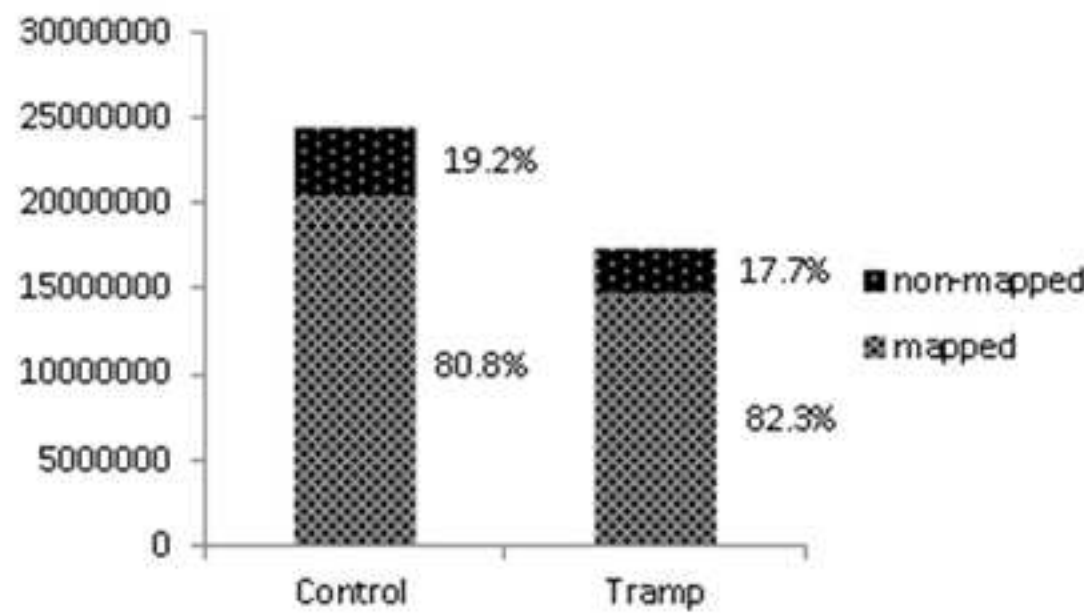
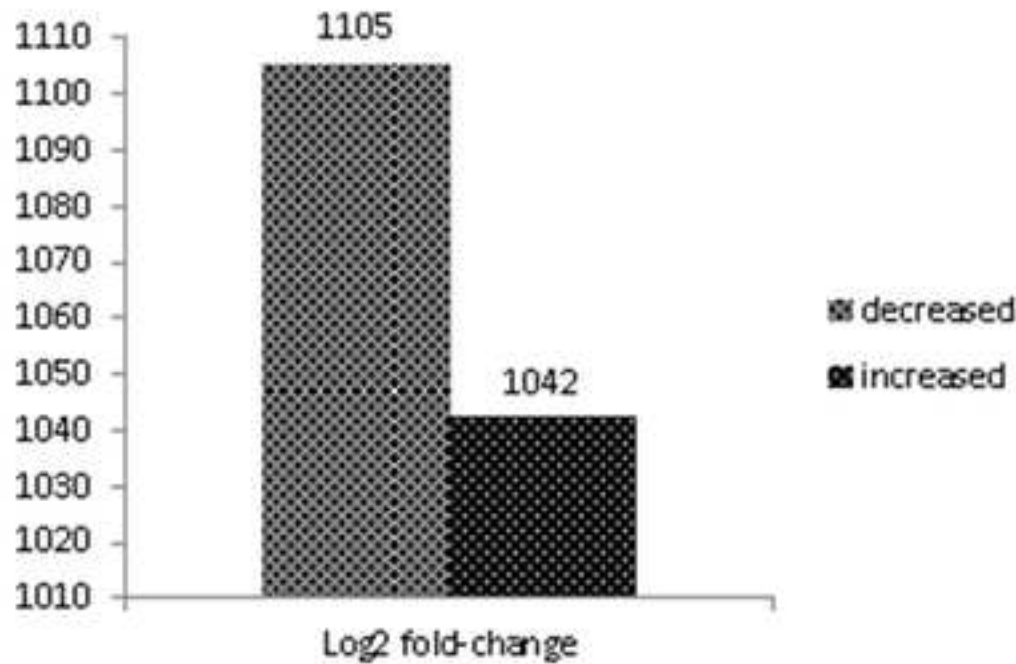
A.**B.**

Figure 2

Click here to download Figure Figure-2.tif

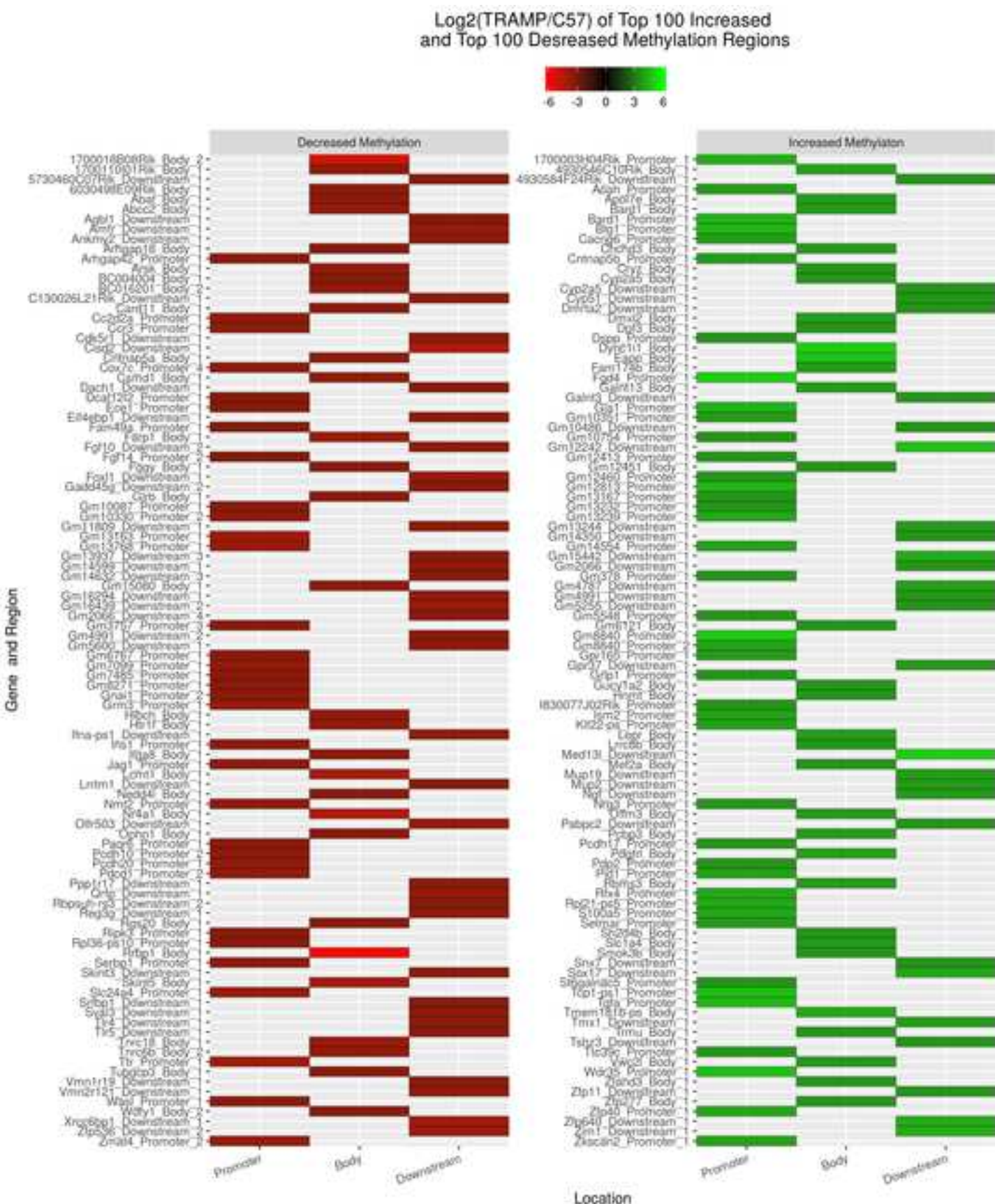
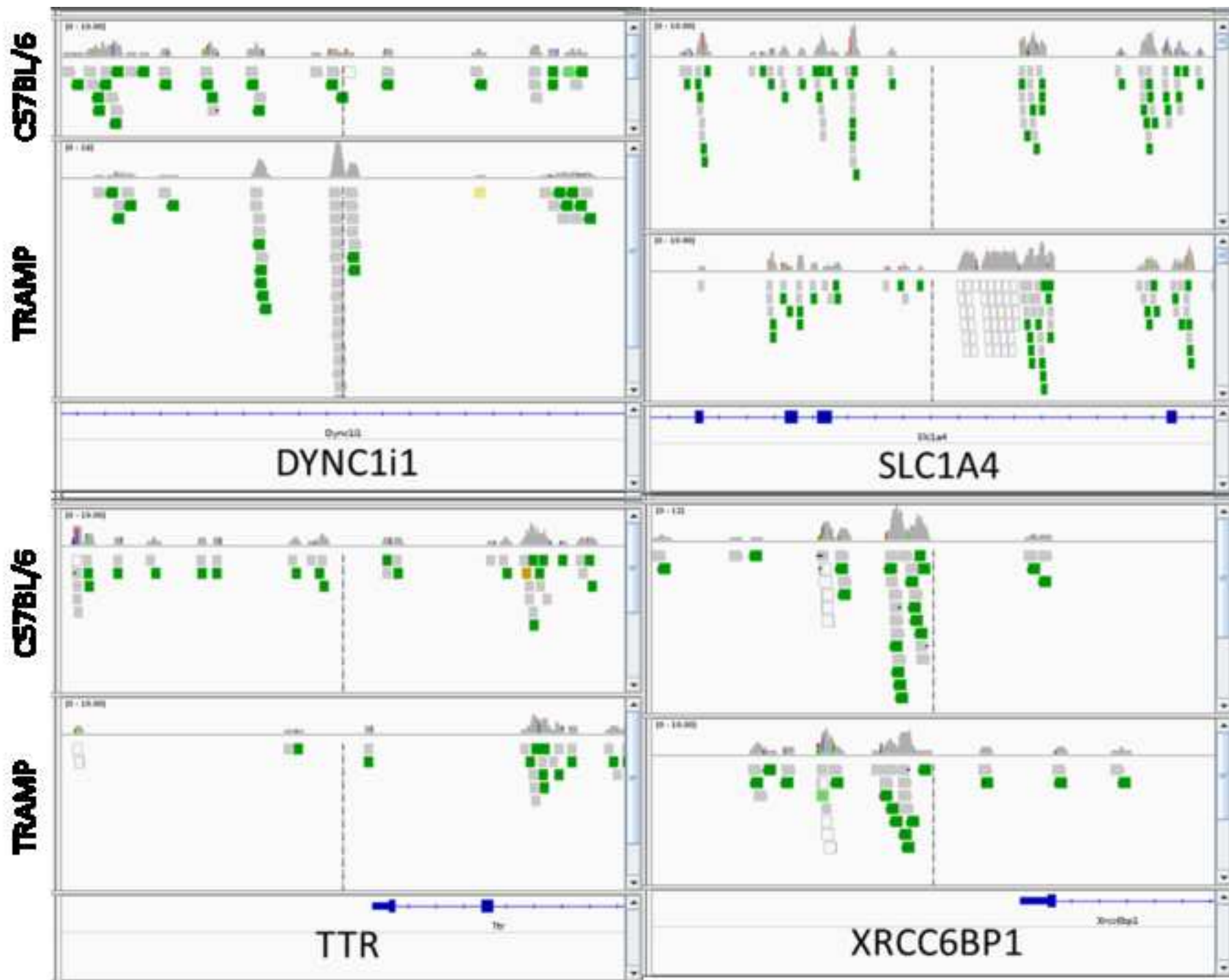


Figure 3

[Click here to download Figure figure-3.tif](#)

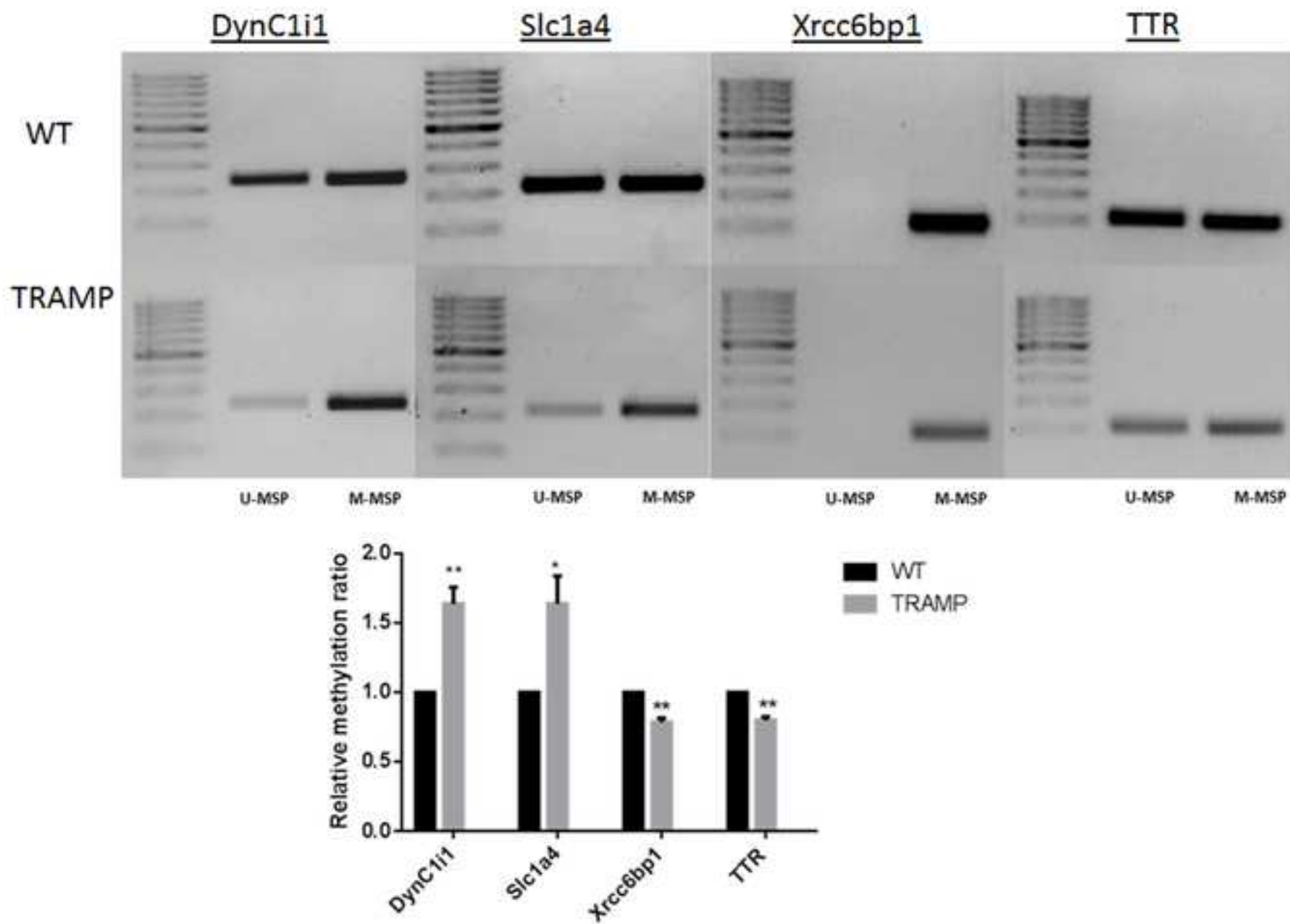
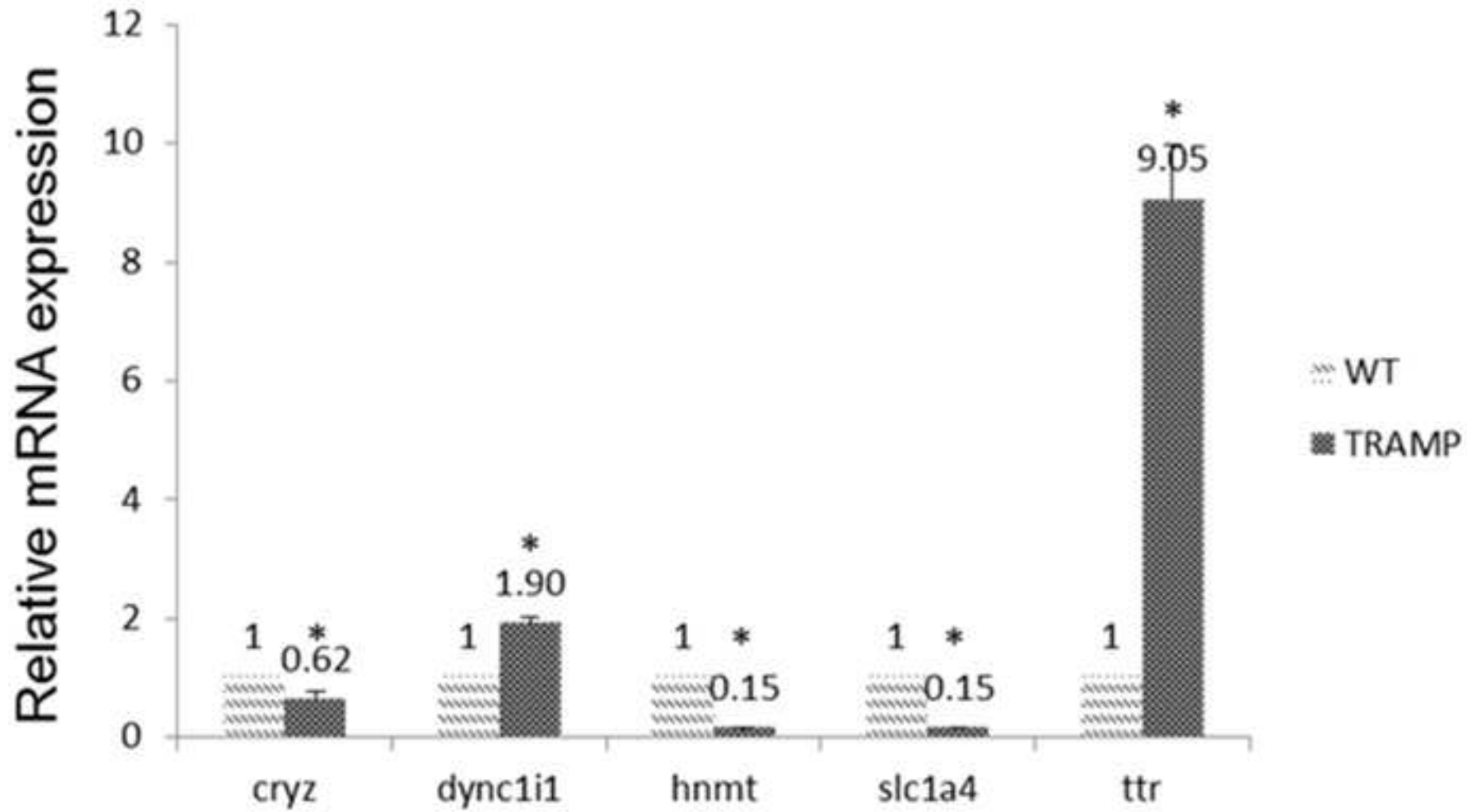
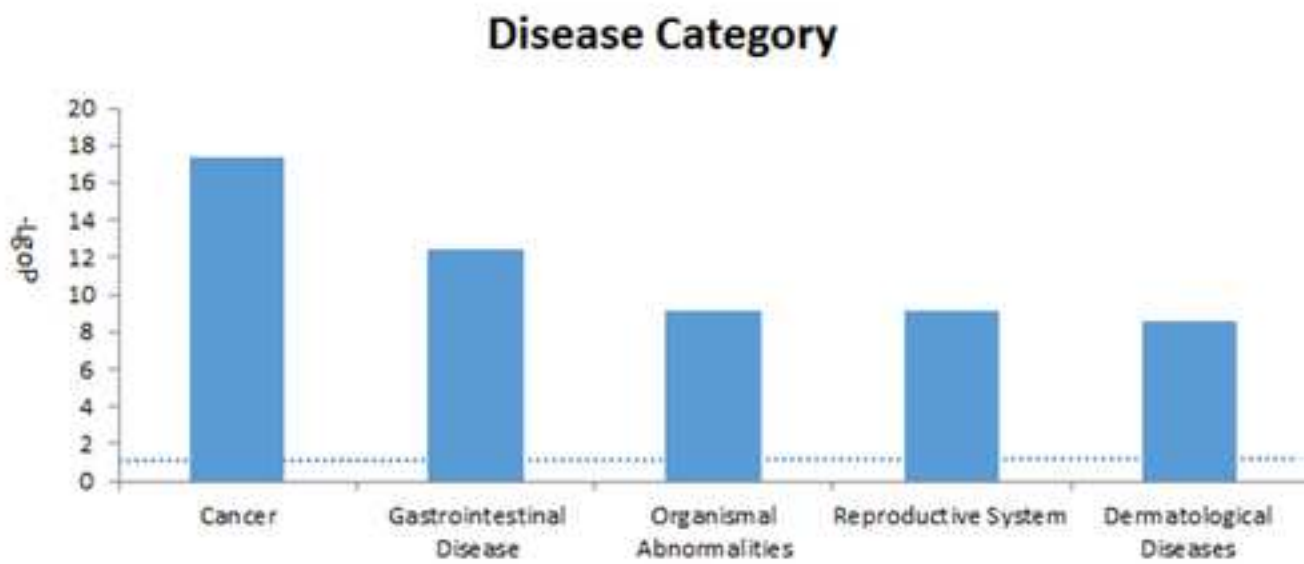


Figure 5

[Click here to download Figure figure-5-300dpi.tif](#)

A



B

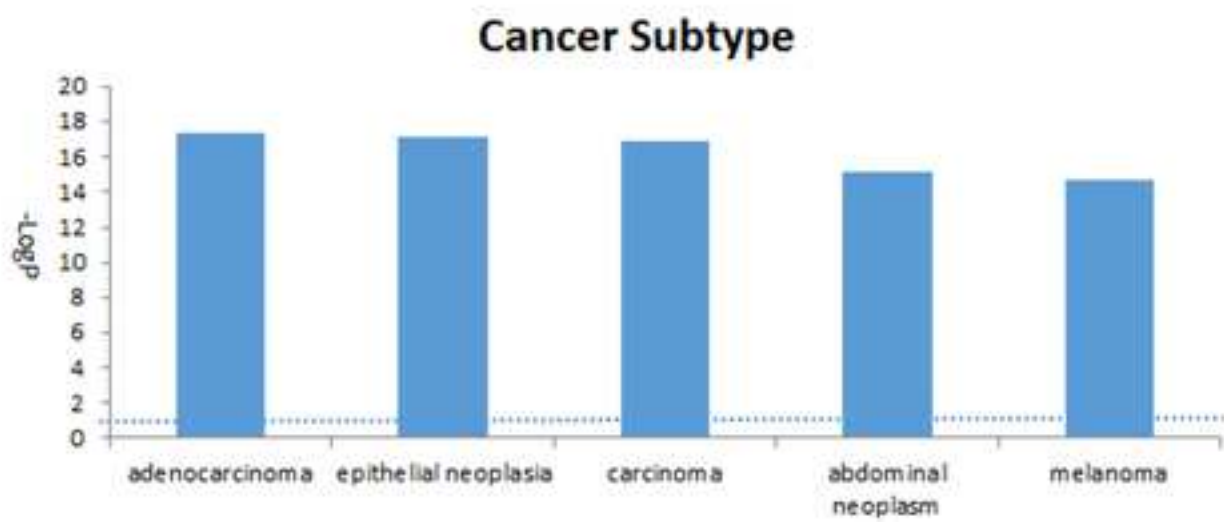


Figure 7

Click here to download Figure figure-7-300dpi.tif

Path Designer Neuropathic Pain Signaling In Dorsal Horn Neurons

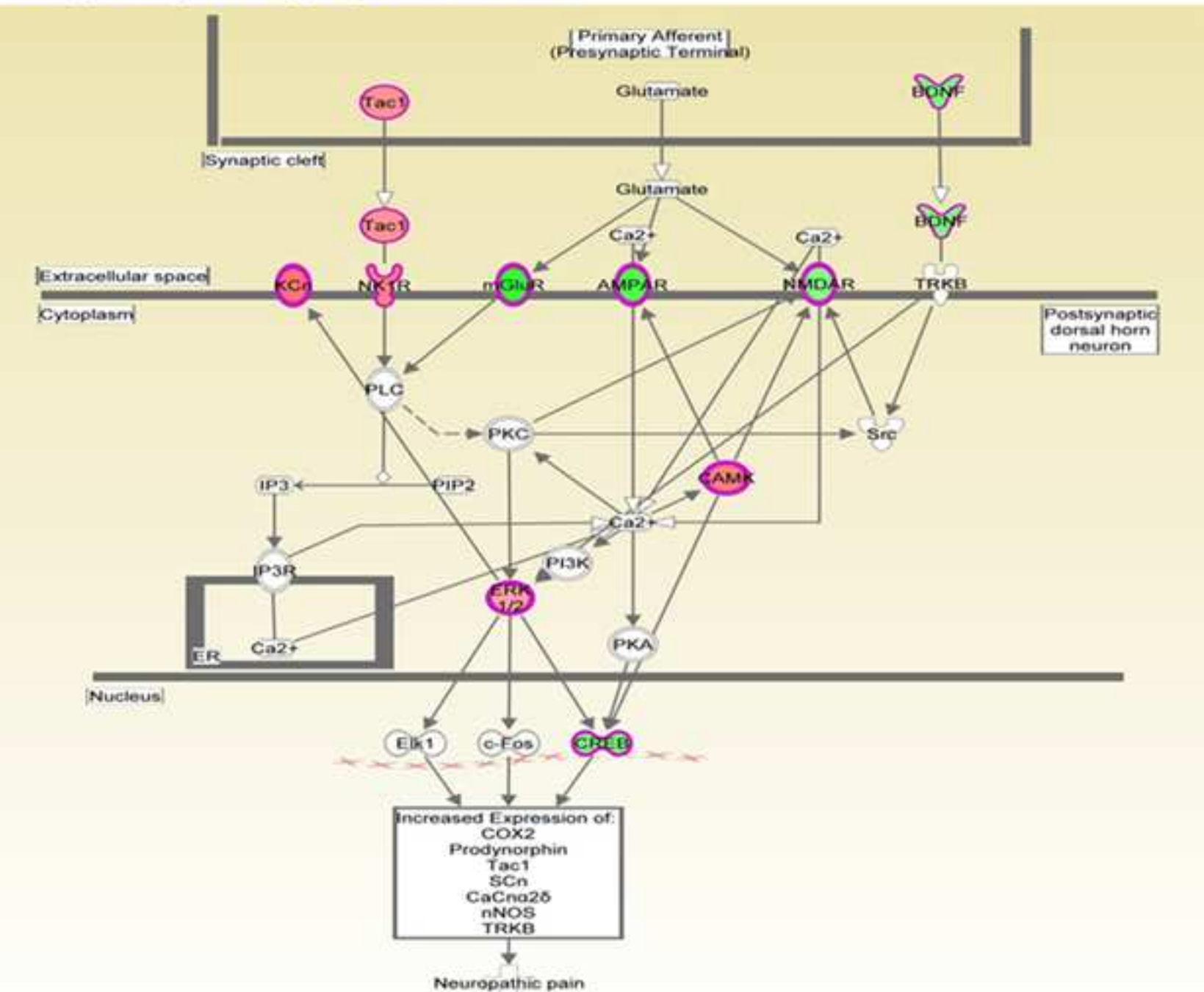


Figure 8

Click here to download Figure Figure 8.tif

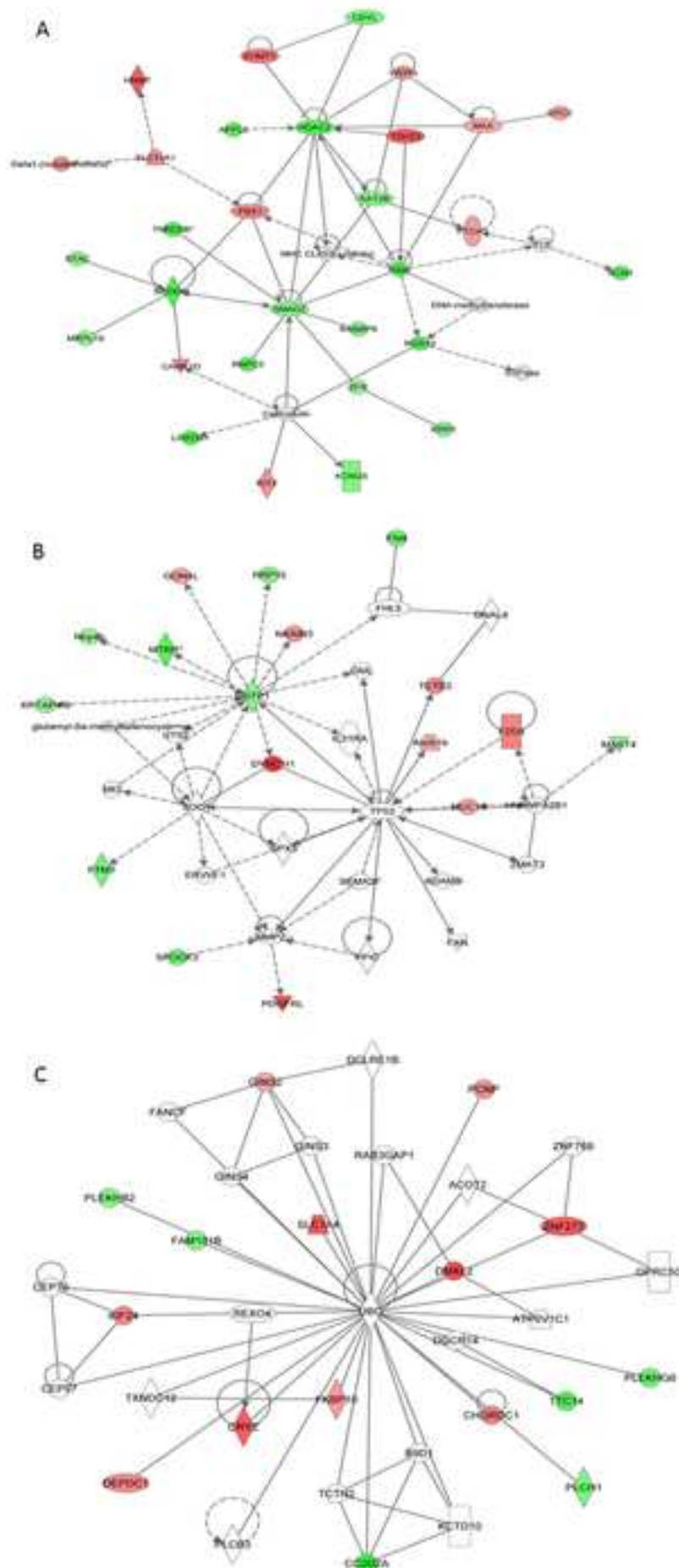
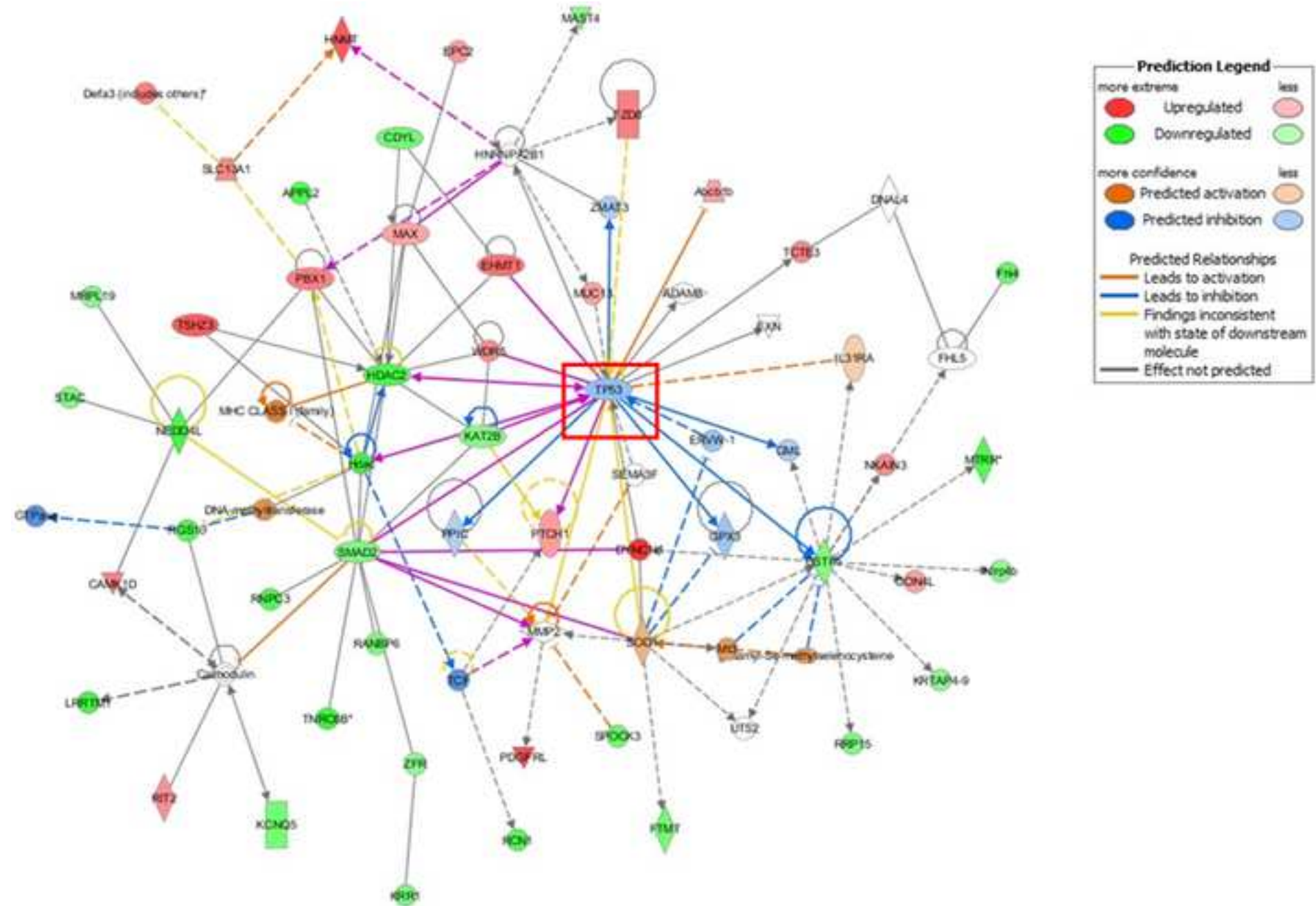


Figure 9

[Click here to download Figure figure-9-300dpi.tif](#)





Click here to access/download
Supplementary Material

Cover Letter_Cell and Bioscience-12-15-17-final.docx